Flavonoid rich fraction of *Oreocnide integrifolia* extract augments genetic reprogramming for islet neogenesis and β-cell regeneration in pancreatectomised BALB/c mice.

Introduction:-

Pancreatic acinar and islet components differentiate by an epithelial-mesenchymal interaction involving a foregut endodermal evagination and the splanchnic mesoderm (Golosow and Grobstein, 1962; Dudek and Lawrence, 1988). During this process, multipotent stem cells differentiate into exocrine and endocrine phenotypes (Lagnesse, 1905; Bensley, 1911; Orci *et al.*, 1979). Islet endocrine cells are purported to develop from embryonic duct like cells by a process of budding resulting in islet morphogenesis in the duct associated mesenchyme (Githers, 1986) and, subsequent orchestrated sequence of gene action lays down the various classes of endocrine cells in the islet. Postnatal and adult β-cells seem to have poor replicative capacity as they are of a terminally differentiated state, with only about 3% of cells exhibiting potential for proliferation (Swenne, 1983; Tanigawa *et al.*, 1997).

Decreased β-cell number or functioning is characteristic of Diabetes mellitus. Whereas an actional reduction in β-cell number by chemical insult or infection is the cause of hypoinsulinemia and type 1 diabetes, diet or obesity induced type 2 diabetes results in initial islet compensation with the consequent effect of decreased β-cell functioning and destruction due to islet decompensation. It is clear by now that, a reduction in β-cell number to a critically low level is correlatable with progression

and outcome of diabetes (Okamoto, 1999; Petrovsky et al., 2002; Risbud and Bhonde, 2002; Zalzman et al., 2003; Yamaoka, 2003). Roughly about 80% of islet cell population is represented by β-cells and the final β-cell mass is established during prenatal life through sequential steps of commitment to pancreatic, endocrine and then β-cell progenitors followed by differentiation and proliferation of specified cells (Bonal et al., 2008). Though, β-cell insufficiency associated with diabetes in general was rectified by islet transplantation (Shapiro et al., 2000; Harlam and Rother, 2004), alternative approaches involved stimulation of regeneration of endogenous pancreatic β-cells. Three different processes targeted to meet this alternative approach include: 1. Proliferation of pre-existing β-cells, 2. Neogenesis from intra-pancreatic progenitor stem cells, and 3. transdifferentiation from pancreatic acinar cells. Experimental induction of β-cell regeneration or neogenesis in diabetic individuals finds basis from the fact that, pancreas has the potential to respond to changes in islet cell mass and regenerate β-cells by a probable intra-pancreatic 'sensing' mechanism (Brockenbrough et al., 1988; Parekh et al., 1991; Wang et al., 1995). There is sufficient evidence for presence of islet stem cells or progenitors in adult pancreas located within or near pancreatic ducts that can under appropriate stimuli differentiate into endocrine cells (Bell et al., 1995; Banerjee and Bhonde, 2003; Hardikar, 2004; Paris et al., 2004). Even other workers have provided evidence for presence of islet progenitor cells and the possible ability of these cells to form mature functional islets in Streptozotocin diabetic mice (Bonner-Weir et al., 2000; Banerjee and Bhonde, 2003; Katdare et al., 2004).

Since, insulin deficiency is the prime basis of all diabetic manifestations, strategies that can trigger β-cell regeneration/ neogenesis would be of pivotal significance in therapy and cure of diabetes. In this behest, agents which can either

310

trigger proliferation of β-cells or induction of neogenesis of β-cells from precursors would be of great merit in reversing diabetic complications. Reports have appeared in recent times regarding inductive agents that have been shown to stimulate regeneration and replenishment of islet cells. Fernandez-Alvarez et al.(2004) have in this context demonstrated stimulated regeneration within pancreas of steptozotocin treated neonatal mice by tungstate. Many other agents like gastro-intestinal neuropeptides, cholecystokinin, natural products and herbal components like fruits of *Terminalia catappa*, extract of *Vinca rosea* and alkaloid extract of *Ephedrae herba* have all been shown to be effective in pancreatic regeneration and enhanced β-cell growth (Ghosh and Suryawanshi, 2001; Xiu *et al.,* 2001; Morisset, 2003; Nagappa *et al.,* 2003).

Our studies with OI extract, in terms of hyperglycemia metabolic alterations, and dyslipidemia, in type 1 and type 2 diabetes models of animals have been encouraging (Chapter 1-4). Hence, it was thought pertinent to evaluate the probable islet regenerative potential of flavanoid rich fraction (FRF) of *Oreocnide integrifolia* in pancreatectomised animal model. To this end, BALB/c mice have been subjected to subtotal pancreatectomy (70%) and the regenerative ability tested by administering FRF to pancreatectomised mice.

Materials and methods:

Animals and operative procedures: partial pancreatectomy

Adult female mice of BALB/c strain around 7-8 weeks old were obtained from Cadila pharmaceuticals, Ahmedabad and acclimatized in the department animal

house for one week. The experiment was carried out according to the guidelines of the Committee for the Purpose of Control and Supervision of Experiments on Animals, India and approved by the Animal Ethical Committee of Department of Zoology, The M.S.University of Baroda, Vadodara (ApprovalNo.827/ac/04/CPCSEA).

Partial pancreatectomy was performed according to the procedures of Bonner Weir et al. (1983) and Hardikar et al. (1999). Briefly, mice were anesthetized using ketamine (150 mg/kg) and xylazine (10 mg/kg) intraperitoneally. A midline abdominal incision allowed exteriorization of the splenic lobe of the pancreas (between the gastroduodenal junction and the spleen). Approximately ~70% percent pancreatectomy was performed by gently denuding the pancreatic tissue from the splenic lobe using cotton-tipped swabs soaked in 0.9% saline, leaving the mesentric pancreas intact. Incisions were closed using 5-0 catgut absorbable sutures (Ethicon), and 3M™Vetbond™ Tissue adhesive. The skin was clipped using 9.0mm skin staples (Leuckoclip SD, Australia) and topical ointment (Soframycin®, Aventis Pharma. Ltd., Pune, India) was applied over the sutured wounds following surgery. Sham operated animals were anesthetized and the pancreas was gently held through the midline incision with cotton applicators for 60 seconds. The skin was sutured as in the case of pancreatectomized animals. All animals (pancreatectomized and sham operated) received an intraperitoneal injection of gentamycin (3 mg/kg body weight), ampicillin (20 mg/kg body weight) and were administered analgesics (Buprenorphine-HCl in normal saline 0.1 mg/kg subcutaneously).

Experimental groups:

The animals were divided into 7 groups, consisting of at least 5 animals each and were sacrificed at predefined time points. Sham operated (S), pancreatectomized groups received 0.5% CMC as vehicle while, Px7+FRF, Px14+FRF and Px21FRF received 250 mg/kg body weight of flavonoidal rich fraction intraperitoneally starting from the day of surgery and sacrificed at day 7(Px 7), day 14 (Px 14) and day 21(Px 21). The experiment was carried out according to the guidelines of the Committee for the Purpose of Control and Supervision of Experiments on Animals (CPCSEA), India and approved by the Animal Ethical Committee of Department of Zoology, The M.S University of Baroda, Vadodara (Approval No. 827/ac/04/ CPCSEA).

Glucose and insulin measurements:

Plasma glucose was measured by the tail-snipping method using One Touch Glucometer (Elegance, USA). Plasma Insulin was quantified according to manufacturer's protocol using Mouse Insulin ELISA kit (Mercodia Diagnostics, Uppsala, Sweden).

In-vivo BrdU pulse labelling /Incorporation

In vivo pulse-labelling with 5-bromo-2-deoxyuridine, a thymidine analogue, and subsequent immunostaining of the incorporated BrdU were carried to mark the cells that synthesized DNA during the incubation time. Six hours before sacrifice, BrdU labelling reagent (100mg/kg body weight, Sigma Aldrich, MO) was injected intraperitoneally into Sham , Px and Px+ FRF groups of animals to label proliferating

313

cells. BrdU stock was prepared in phosphate buffered saline (PBS), (pH 7.2, 0.1 M) with 0.1 N NaOH at 20 mg/ml. After sacrifice, a portion of the pancreas from the same anatomical location, including the main pancreatic duct, was immediately fixed in 4% paraformaldehyde buffered with 0.01 mol/L sodium phosphate, pH 7.4 (PBS) overnight at 4 degree C, dehydrated with ethanol and embedded in paraffin wax.

Haemetoxylin and Eosin staining:

Pancreatic tissue sections were incubated at 60°C for 10 min, deparaffinated in xylene and then stained with hematoxylin (Sigma-Aldrich, St Louis,USA).Sections were then dehydrated using gradients of ethanol and finally in100% ethanol before staining with Eosin Y (Hi-Media Labs, Mumbai, India). Slides were then rehydrated by downgrading them in ethanol and mounted in DPX. Images were captured using Leica DMRB binocular microscope with digital camera.

Immunohistochemistry and Confocal Microscopy

Five microns thick serial sections were mounted on Poly-L-lysine (Sigma Aldrich, MO, USA). For immunohistochemical detection of BrdU-incorporating nuclei, DNA was first denatured to expose the antigen by incubating the tissue sections in 1N HCl for 45 min at 45°C. The sections were rinsed three times for 5 min each in PBS, then incubated with primary antibodies to Mouse monoclonal BrdU (1:200 Sigma Aldrich, MO,USA), Guinea pig anti insulin (1:200; Invitrogen, USA,) Rabbit Pdx-1 polyclonal (C terminus raised; 1:400, Millipore) in 0.1% Triton-X solution in antibody diluent solution), for 12 h at 4°C. For Pdx-1, antigen unmasking

314

step was performed in microwave using Sodium citrate buffer. Non-specific blocking was performed using 4% normal donkey serum and 1% BSA. Next, the labelled sections were washed with PBS (3 times at 5 min each) and secondary incubation was carried out in the dark for 2 hr at room temperature. For the secondary incubation, appropriate fluorochrome-conjugated secondary antibody (Alexa–Fluor 488 and Alexa–Fluor 546F (ab') 2 secondary antibodies (Molecular Probes, OR, USA) were used at 1:200 dilution. DAPI was used to visualize nuclei. Negative controls were run where the primary antibody incubations were omitted. After 2 hr, the tissue sections were washed in calcium magnesium containing PBS, and mounted with anti-fade mounting medium Vectasheild (Vector Laboratories, Burlingame, CA). The slides were allowed to air dry in the dark at room temperature and then stored at 4°C until used for analysis.

A laser scanning confocal microscope, model LSM 510 META (Carl Zeiss, Germany), fitted with an Axiovert 100M microscope (Carl Zeiss) was used with a 63X1.4NA pan Apochromat objective (Carl Zeiss). Excitation on the laser scanning confocal microscope was with a 15 mW argon ion laser emitting at 488 nm, a 1.0-mW helium/neon laser emitting at 543 nm, and 5.0mW helium/neon laser emitting at 633 nm. Emissions were captured using a 505- to 530-nm band pass filter to collect Alexa green emissions and 560- to 615-nm band pass filter to collect Alexa red emissions with optical Z sections ~0.8 microns. Magnification, laser and detector gains, pinhole settings were set below saturation and were identical across samples.

Morphometry and Image Analysis:

For proliferation index of BrdU labelled cells, number of BrdU$^+$ cells per islet was counted in the insulin positive or glucagon positive area. At least 10 islets per animal from non-overlapping areas were counted and islets of less than 100 microns were considered as small islets while, those that were more than 100 micrometer in size were considered as large islets. Acinar cell proliferation analysis was performed by randomly acquiring five DAPI/BrdU areas of acinar cells from each section. Acinar cells were counted for total BrdU$^+$ and total DAPI$^+$ nuclei in day 7. Individual animal results of pancreatic acinar tissue each represent 10 fields counted per animal BrdU incorporation in ducts was also counted in day 7. Ducts less than 100 microns (internal diameter) were considered small duct while, those of 100-300 microns were considered large ducts. Number of ducts giving rise to islets was counted using H&E staining and classified as large and small ducts based on internal diameter.

Quantitative Real Time PCR:

Pancreas was homogenized in Trizol® (Invitrogen, Carlsbad, CA) and RNA was isolated as per the manufacturers' instructions, measured on ND-1000 spectrophotometer (NanoDrop Technologies, Wilmington, DE) and taken for reverse transcription / duplex Taqman® based probe quantitative real-time pcr. First strand cDNA synthesis was carried out using 'high capacity cDNA archive kit' (Applied Biosystems, Foster City, CA). PCR was performed in 10 µl total volume in 96-well plates using cDNA prepared from 100 ng of total RNA on a 7500 FAST real time PCR cycler (Applied Biosystems, Foster City, CA). Primers and probes were Assay-on-Demand (Applied Biosystems, Foster City, CA). All qRT-PCR results are normalized

to 18S (VIC-labelled) ribosomal RNA carried out in duplex reaction (with FAM labelled target gene probes) to correct for any differences in RNA input. All PCR reactions were analyzed after 35 cycles of reaction. The $\Delta\Delta$ Ct method of relative quantification was used to determine the fold change in expression. This was achieved by first normalizing the resulting threshold cycle (Ct) values of the target mRNAs to the Ct values of 18S internal control of the same sample ($\Delta Ct = Ct_{target} - Ct_{18S}$). It was further normalized with the experimental control ($\Delta\Delta Ct = \Delta Ct_{target} - \Delta Ct_{control}$). The fold change in expression was then obtained ($2^{-\Delta\Delta Ct}$).

Results:

Plasma glucose and insulin levels:

Pancreatectomised mice entered into a phase of significant hyperglycaemia within one week, which persisted even at three weeks. Pancreatectomised mice treated with FRF extract showed significantly lower hyperglycaemia, which showed a slow but gradual decline through one to three weeks (Fig. 1). Plasma insulin level which was significantly low one week after pancreatectomy showed a gradual increase through weeks two and three. Though there was no significant difference in plasma insulin titre of Px FRF mice at week one and two compared to Px, during the third week, the insulin level showed noticeable increase compared to Px animals (Fig.2).

Histological observations (Fig. 3 A- Z1):

Evaluation of routine HE stained sections of pancreas reveals bunch of endocrine cells budding off from small pancreatic ductules by day 7 of Px (Fig. 3 C-F). Duct associated vascular channels are also visible in the neighbourhood of budding endocrine cells. By day 14 (Fig. 3 G-L), the budded off chumps of endocrine cells appear as well organised larger islets. By day 21 (Fig. 3 M, N), the newly formed islets have acquired normal looking demarcated islets that seemed to be sinking into the nearby acini.

FRF treated pancreatic remnants seem to show more prominent islet like buds getting organised around pancreatic ducts by day 7 (Fig. 3 O-T) with, increased cell density, probably by way of proliferation of ductal precursor cells. Relatively more number of buds seems to be originating in FRF treated pancreas. Clear association

318

with vascular channels is also visible. By 14 day post Px (Fig. 3 U-Z), FRF treated mice seem to show very prominent and relatively greater acinar organisations with prominent ductal epithelia. By day 21 (Fig. 3 Z 1), well organised islets between acini in the vicinity of ducts are visible. The FRF treated pancreas in general seems to show relatively more number of islet neogenesis.

BrdU incorporation and glucagon, insulin and BrdU labelling:

Immunostaining for glucagon, insulin and BrdU revealed relatively fewer glucagon positive cells than insulin positive cells and relatively greater Co-BrdU labelling with insulin cells and acinar cells than with glucagon cells.

In terms of BrdU incorporation, glucagon positive cells showed equal degree of proliferation in both Px and Px + FRF pancreas. Almost same was the case even for acinar cells, though an insignificantly higher incorporation was the feature in Px + FRF pancreas. In contrast, both insulin reactivity as well BrdU labelling seemed to be higher in general compared to α-cells and acinar cells but with a significantly higher reactivity and labelling in Px + FRF pancreas through week 1 to week 3 post Px. There was significant temporal increase in insulin immunostaining, which was more prominent in Px + FRF pancreas. An overall quantitative evaluation of BrdU incorporation in terms of percentage incorporation revealed a temporal increase across all sizes of islets (Fig. 8) with a significantly greater incorporation in Px + FRF pancreas. Insulin immunoreactivity along with BrdU incorporation in ducts (Fig. 11) by day 7 showed clearly increased BrdU labelling and higher insulin positive cells in the islet budded off from the duct. A quantitative estimate of BrdU label in the ducts revealed significantly higher labelling in Px + FRF than in Px pancreas. In

comparison, smaller ducts seemed to show relatively higher labelling than the larger ducts.

Immunolabelling of Pdx-1 and insulin (Fig. 7):

Both Px and Px + FRF showed significant increment in insulin and Pdx-1 immunoreactivity seven days post Px. In comparison, Px + FRF pancreatic acini show significantly greater immunoreactivity than Px acini.

Proinsulin 1 and 2 transcripts (Fig. 12, 13):

Both the proinsulin transcripts showed a significant decrement seven days post Px with a relatively lesser decrement in Px + FRF pancreas. Expressions are increased gradually over 14 and 21 days post Px with relatively greater expression in FRF treated pancreas.

Reg 3-α and Reg3-γ transcripts (Fig. 14, 15):

Both Reg 3-α and Reg3-γ transcripts were over-expressed maximally at day 7 post Px with FRF treated mice pancreas showing significantly greater expression. Both the transcripts decreased gradually to reach lowest levels by day 21 post Px with the levels in Px +FRF being relatively higher at all times.

Pdx-1 and Ngn-3 transcripts (Fig. 16, 17):

Upregulated expression of both transcripts were the feature at day 7 post Px with relatively greater expression in Px + FRF mice pancreas. Transcript levels of both genes decreased thereafter through day 14 to reach the lowest levels at day 21, with the transcript levels in Px+ FRF pancreas being relatively higher at all time periods.

Fig. 1 Effect of FRF on plasma glucose levels 21 days post Px

Blood Glucose

• = p < 0.05, ■ =p <0.01, ◆ =p < 0.001:sham was compared to other experimental groups
α = p <0.05, β = p <0.01, δ = p <0.001: Px day 7 was compared to Px day 7 + OI
① = p <0.05, ② = p< 0.01, ③ = p < 0.001: Px day 14 was compared to Px day 14 + OI
❶ = p <0.05, ❷ = p <0.01, ❸ = p <0.001: Px day 21 was compared to Px day 21 + OI
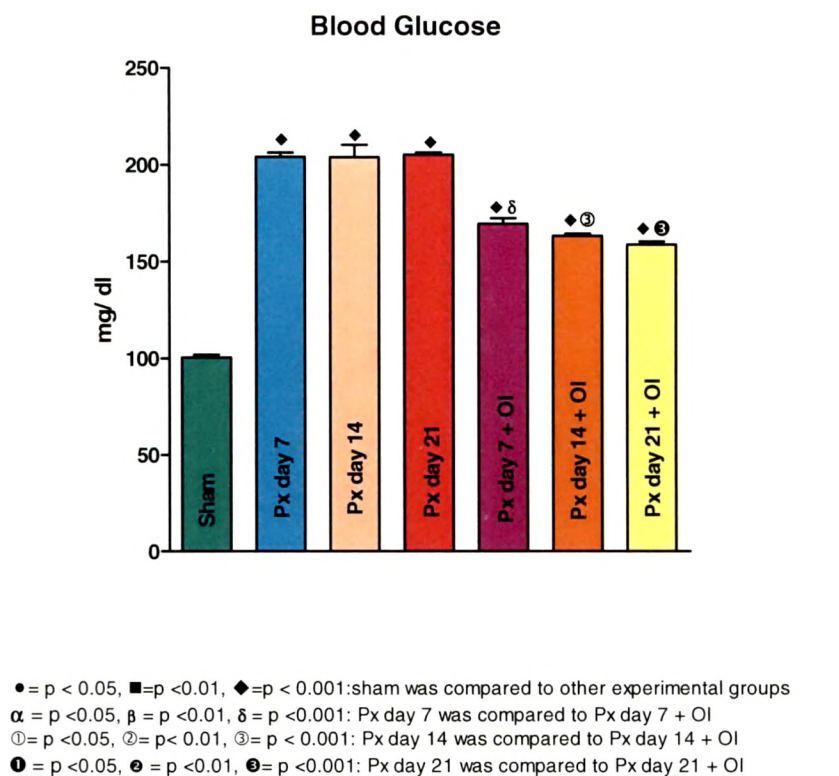
Fig. 2 Effect of FRF on plasma insulin levels 21 days post Px

Plasma Insulin

• = p < 0.05, ■ =p <0.01, ◆ =p < 0.001:sham was compared to other experimental groups
α = p <0.05, β = p <0.01, δ = p <0.001: Px day 7 was compared to Px day 7 + OI
① = p <0.05, ② = p< 0.01, ③ = p < 0.001: Px day 14 was compared to Px day 14 + OI
❶ = p <0.05, ❷ = p <0.01, ❸ = p <0.001: Px day 21 was compared to Px day 21 + OI
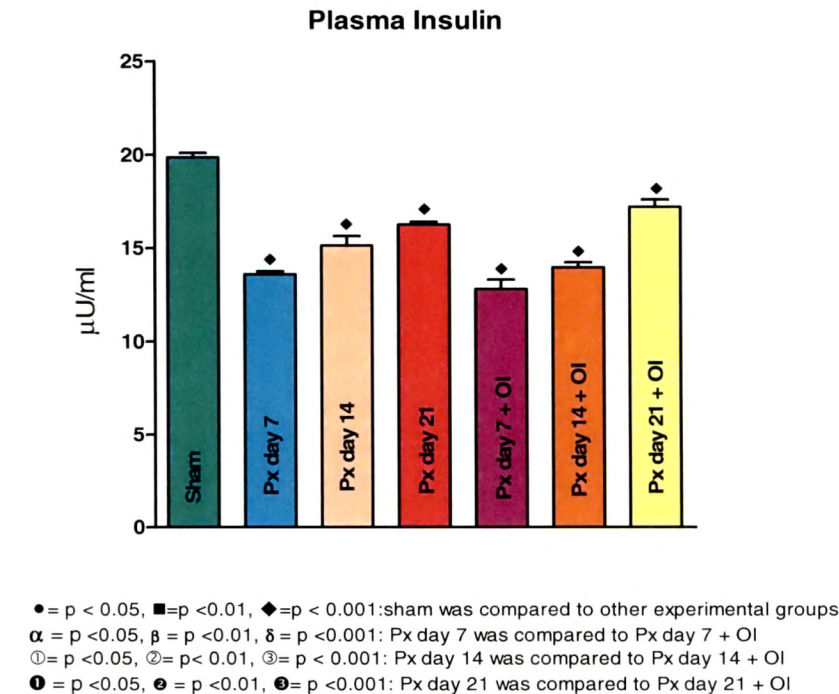
Fig. 3 A and B: Photomicrographs of Sham operated mice showing

normal looking islets with compactly packed cells (450 x).

Fig. 3 HAEMATOXYLIN AND EOSIN STAINING OF PANCREAS
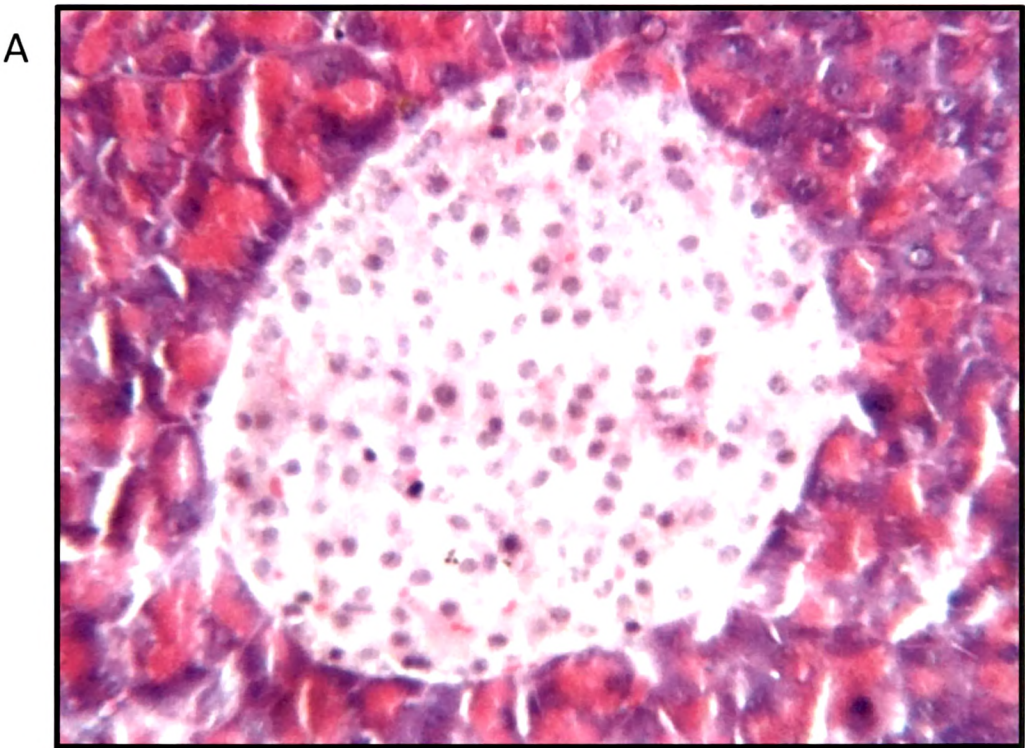
CONTROL
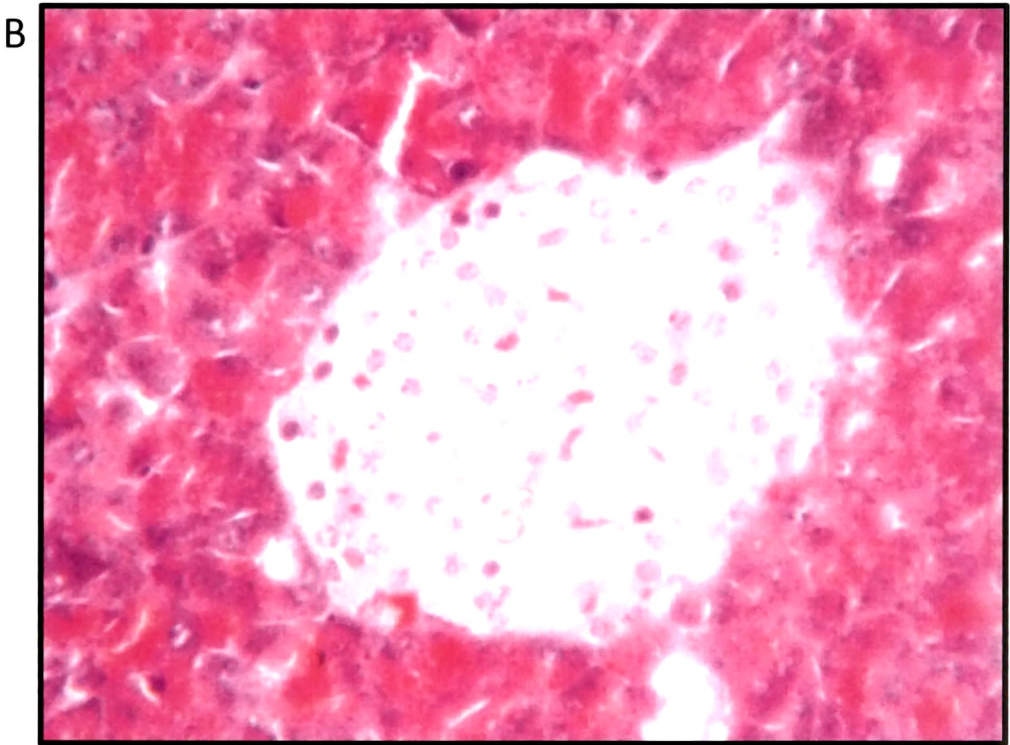
CONTROL

Fig. 3 (C - F): H&E stained sections of pancreas on day 7 post Px

showing islet neogenesis in association with ducts. Note the islet like

aggregations in contact with ducts suggesting ductal origin (450 x).

Fig. 3 HAEMATOXYLIN AND EOSIN STAINING OF PANCREAS

C
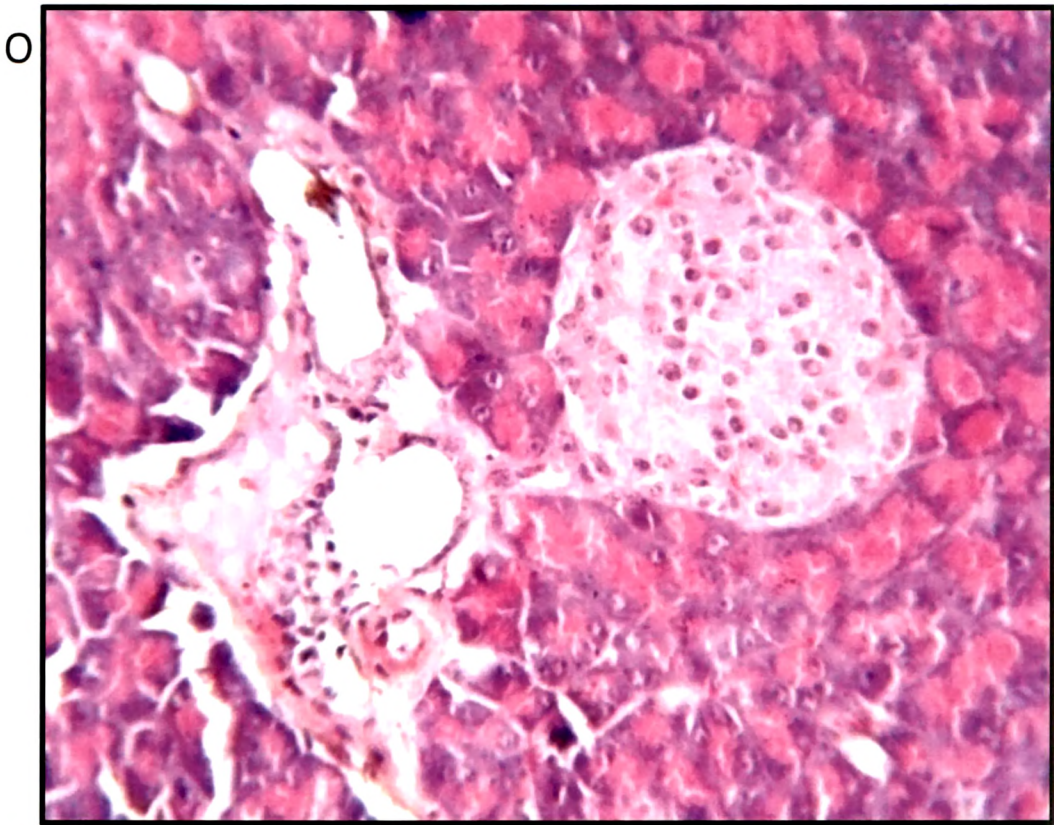

Px day 7

D
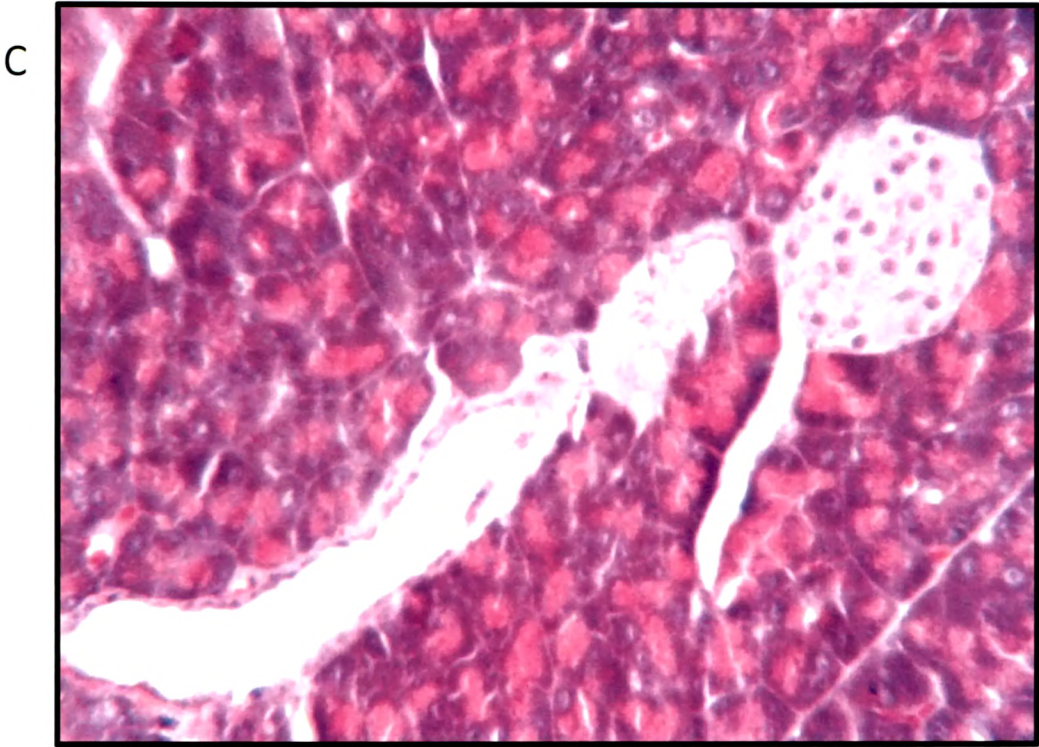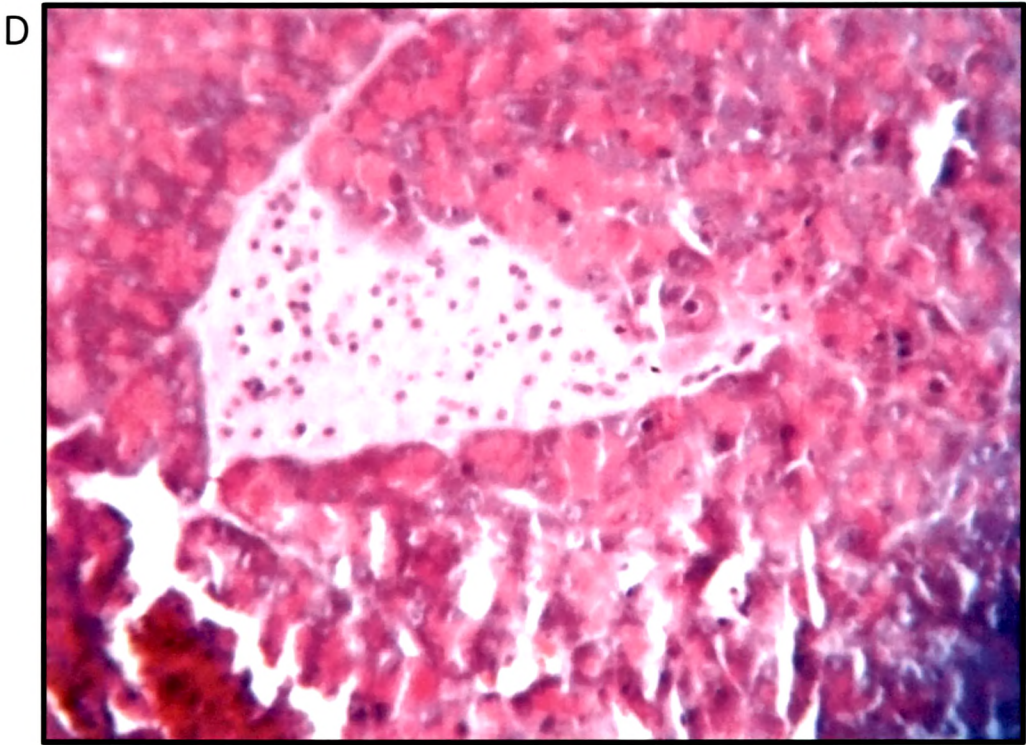
Px day 7

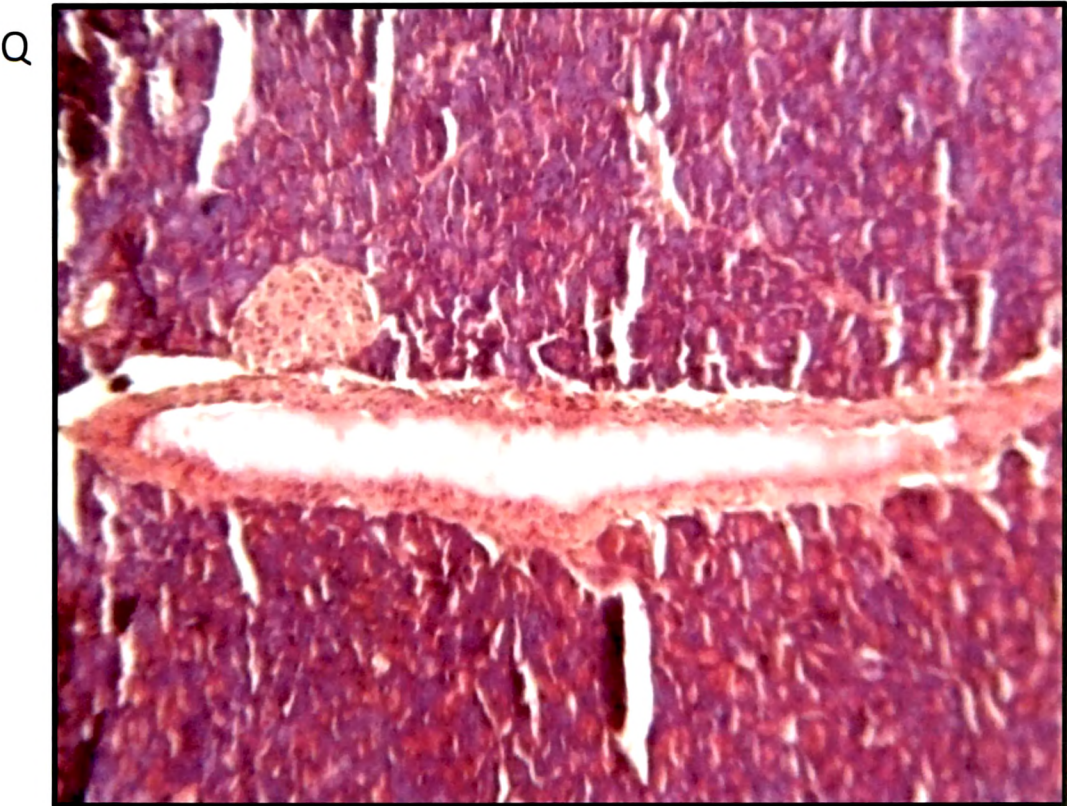## Fig. 3 HAEMATOXYLIN AND EOSIN STAINING OF PANCREAS

E

Px day 7

F
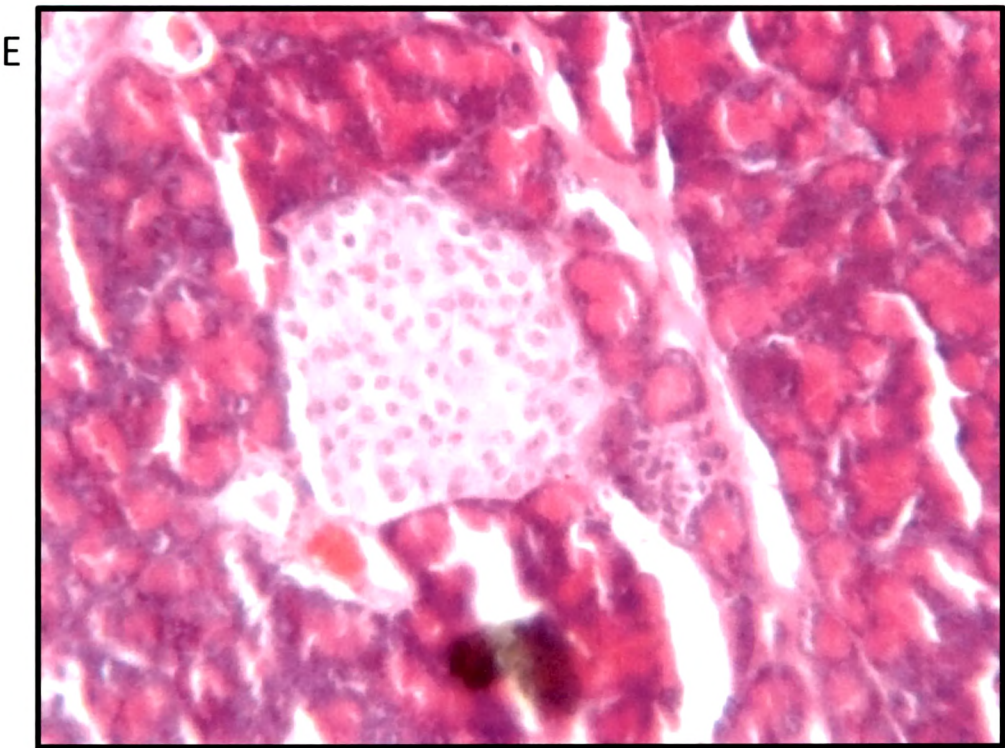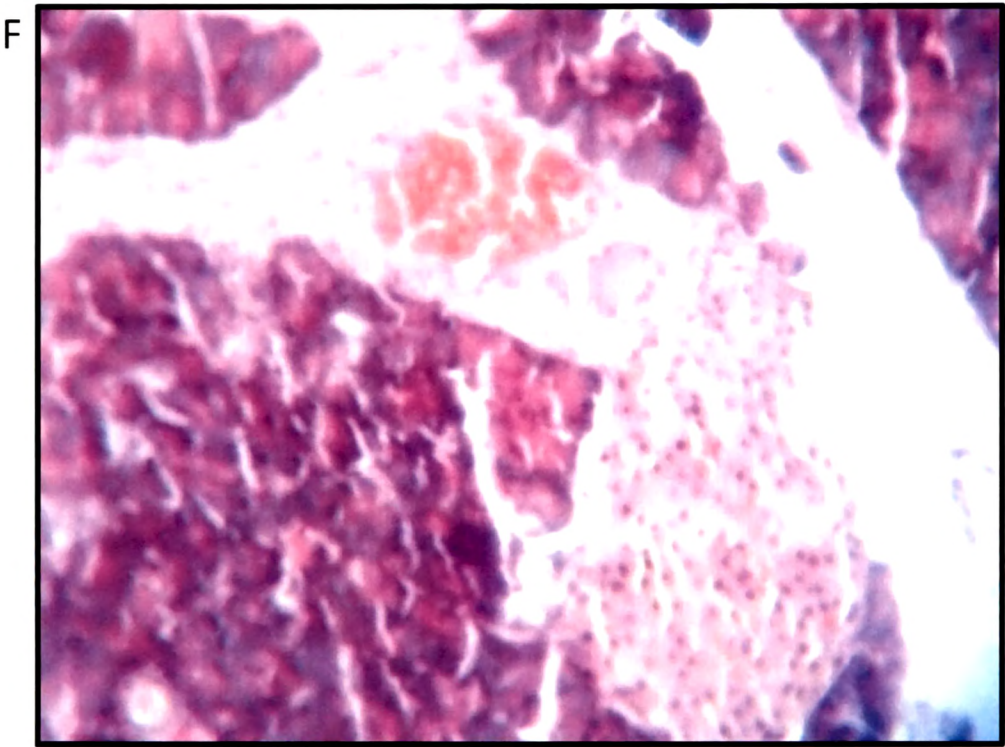
Px day 7

Fig. 3 G and H: Day 14 post Px pancreas showing well formed islets still in contact with ducts (G: 100x; H: 450x).

Fig. 3 HAEMATOXYLIN AND EOSIN STAINING OF PANCREAS

G

Px day 14

H
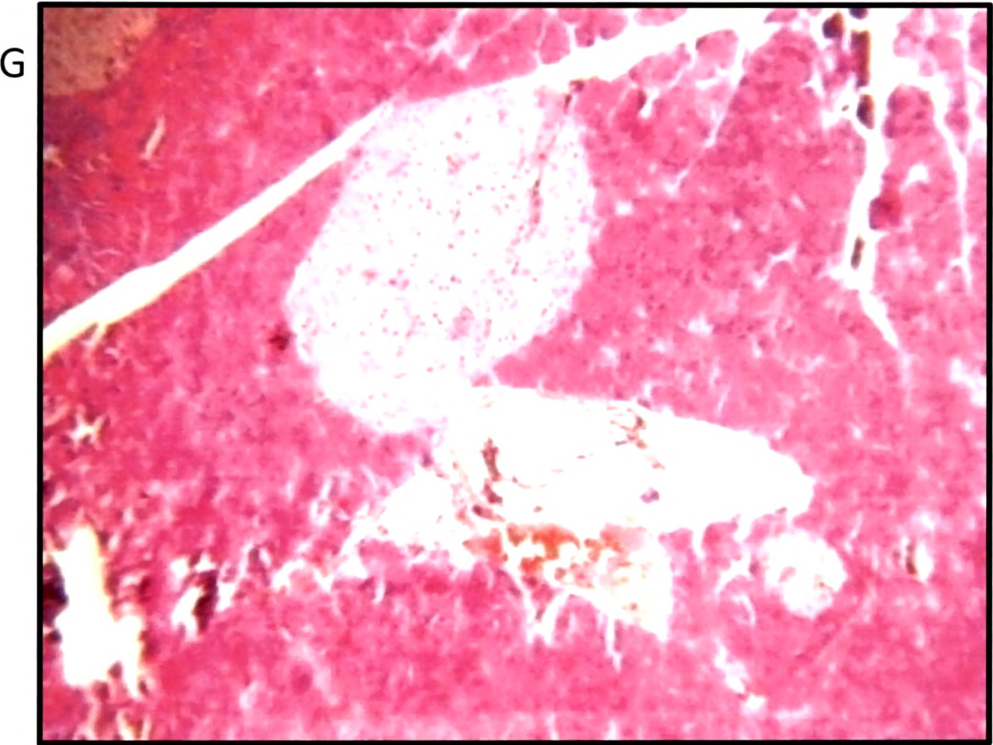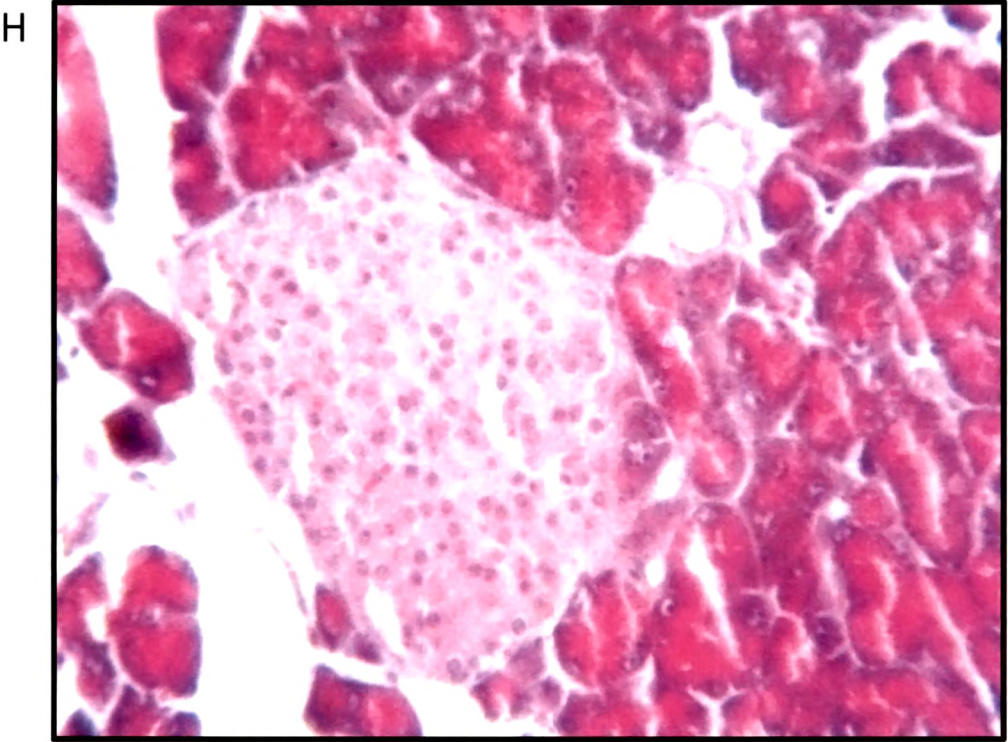
Px day 14

Fig. 3 I and J: Sections of day 14 post Px pancreas showing pancreatic ducts with proliferating neogenic islet cells (I: 100 x, J: 450 x, magnified view).

Fig. 3 HAEMATOXYLIN AND EOSIN STAINING OF PANCREAS

I

Px day 14

J
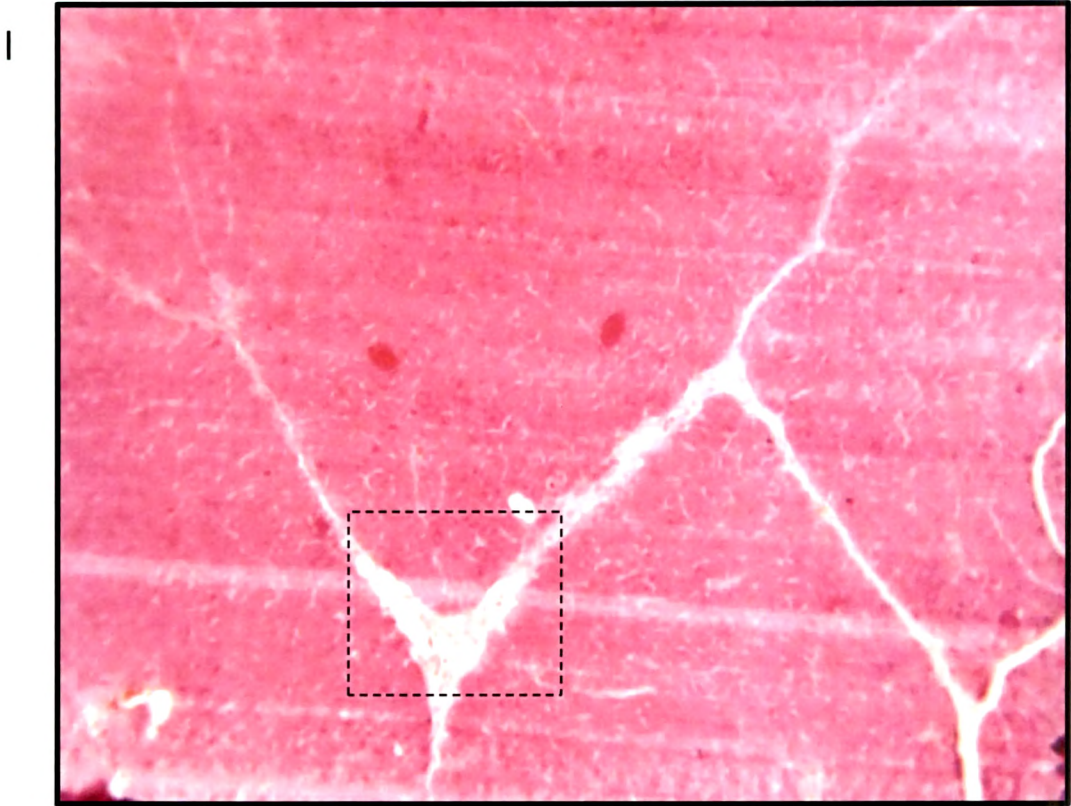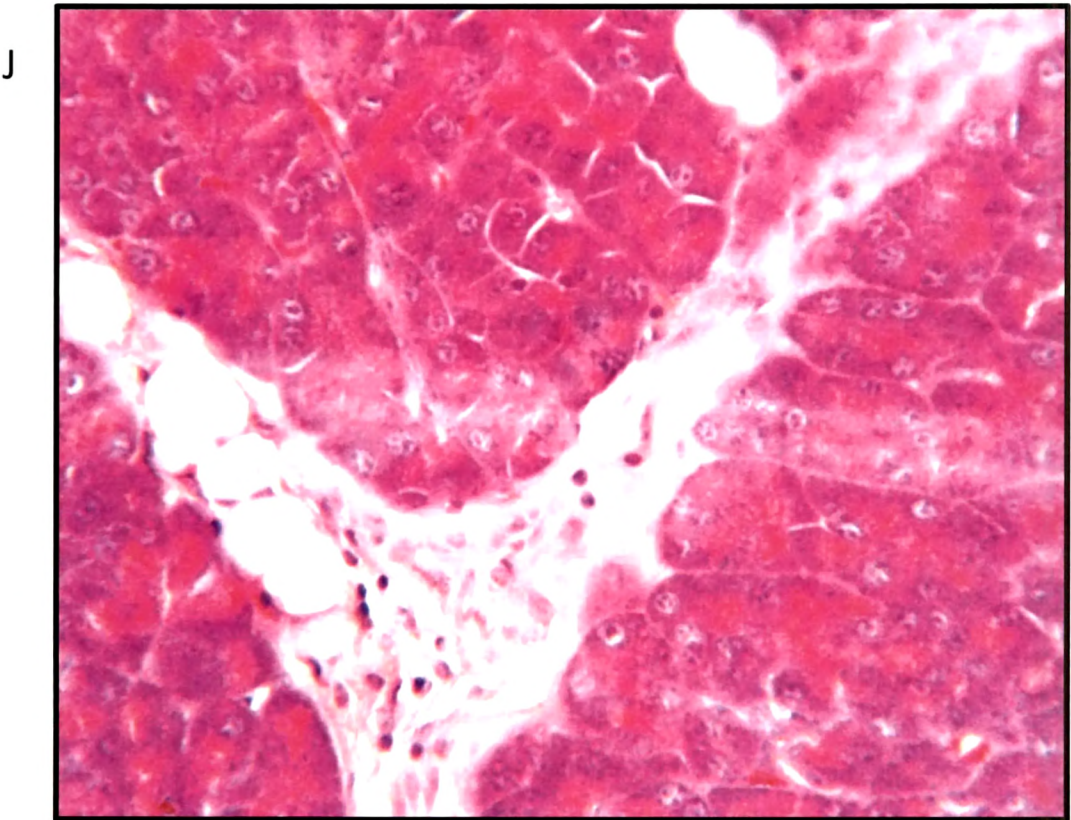
Px day 14

Fig. 3 K and L: More sections of day 14 post Px pancreas showing duct

associated neogenic islets (450 x).

Fig. 3 HAEMATOXYLIN AND EOSIN STAINING OF PANCREAS

K
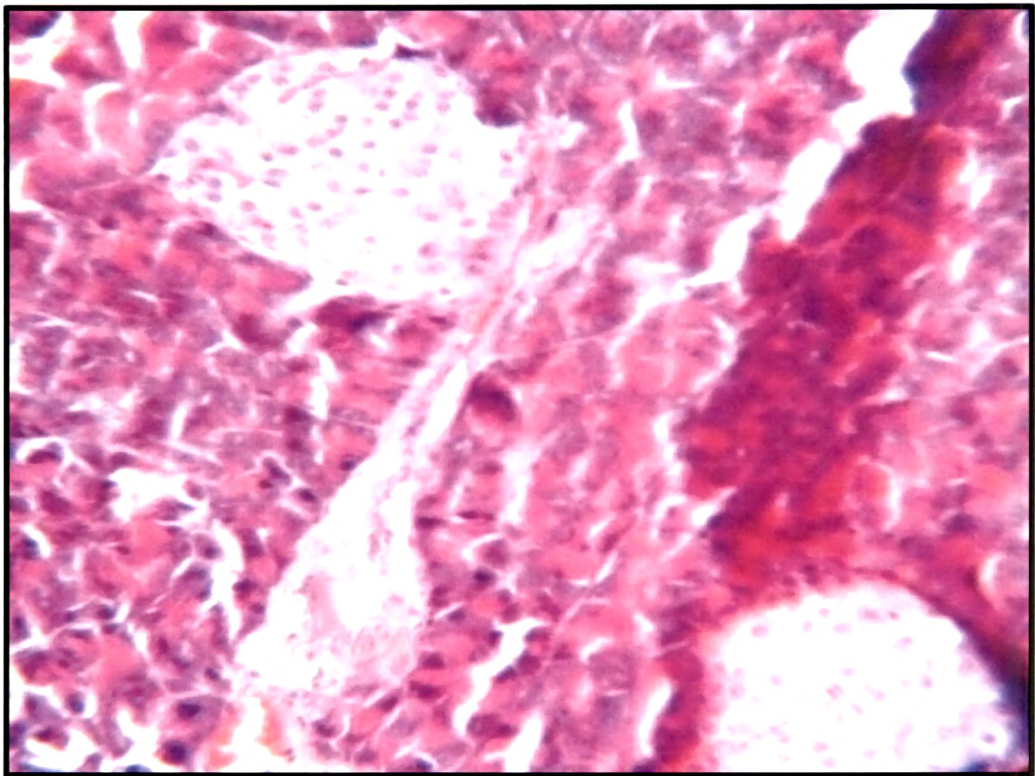
Px day 14

L
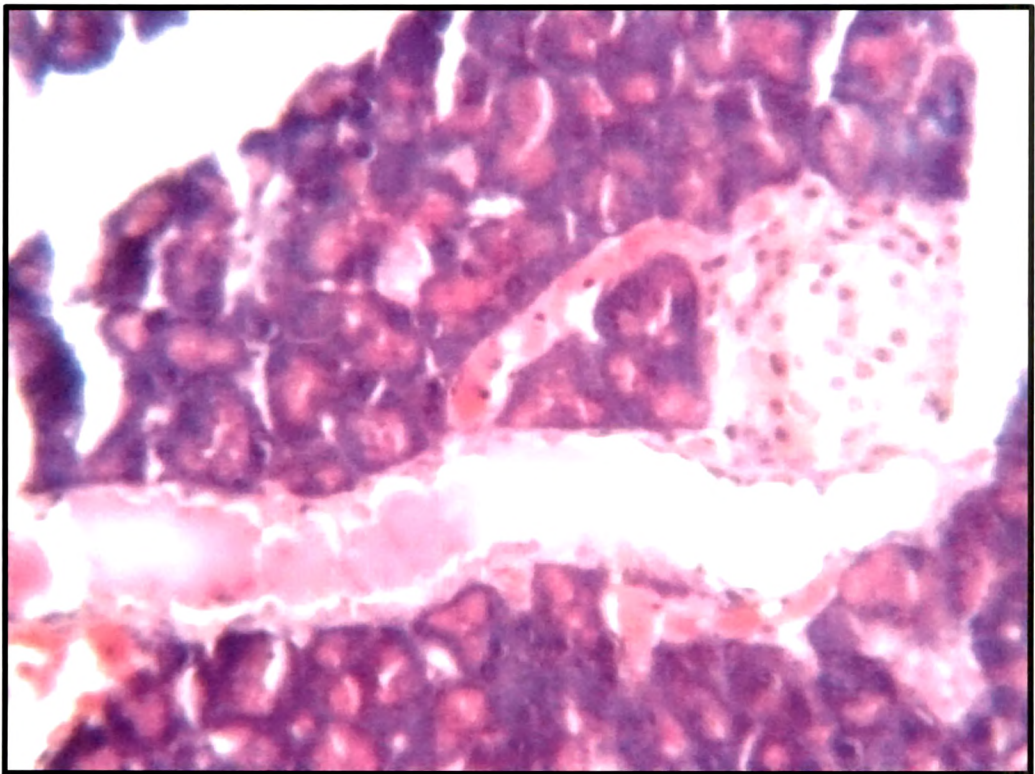
Px day 14

Fig. 3 M and N: Sections of pancreas 21 days post Px showing many

neogenic islets, budded off from the ducts and lying within the acini

(100 x).

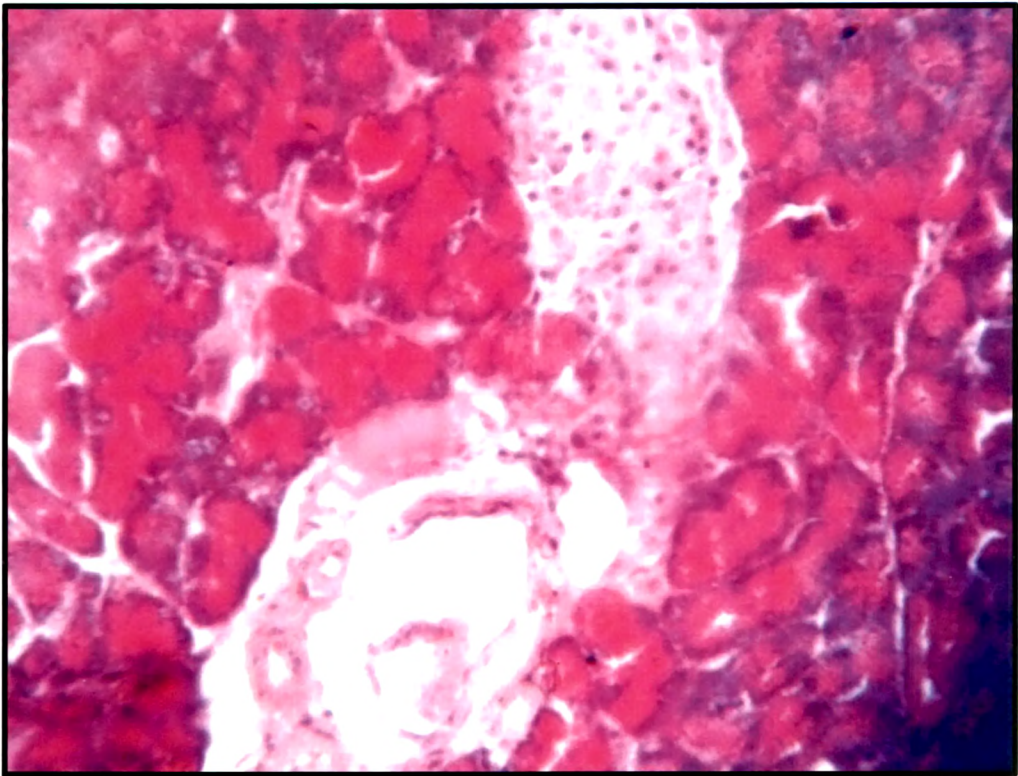# Fig. 3 HAEMATOXYLIN AND EOSIN STAINING OF PANCREAS

M

Px day 21

N
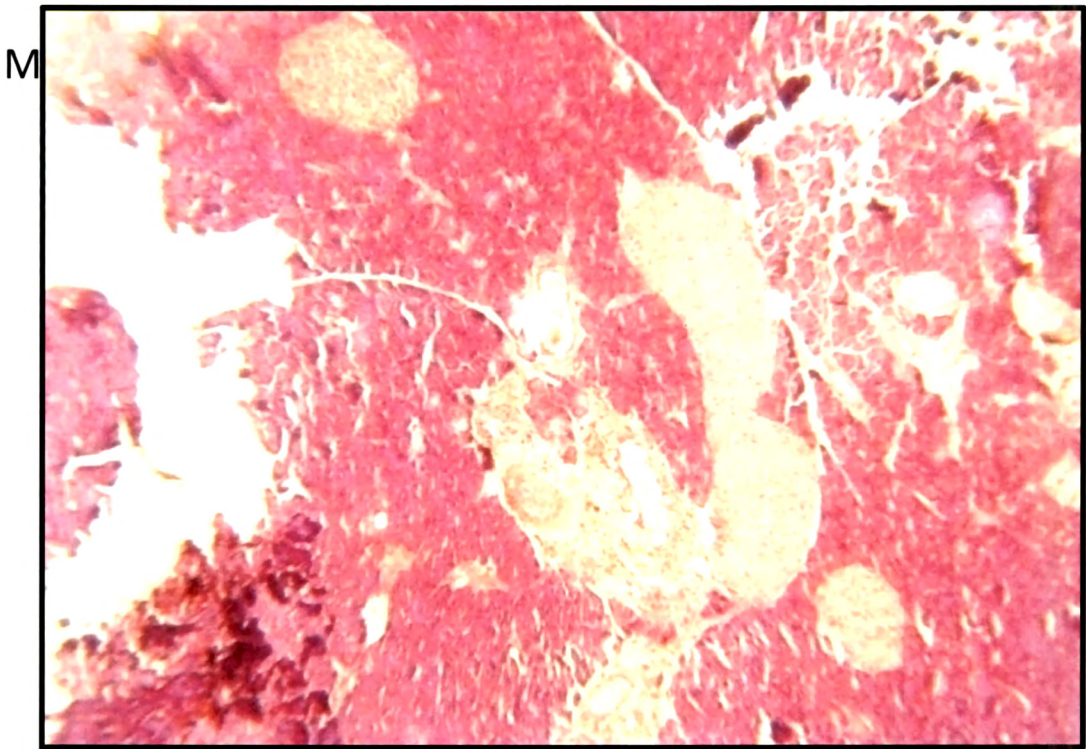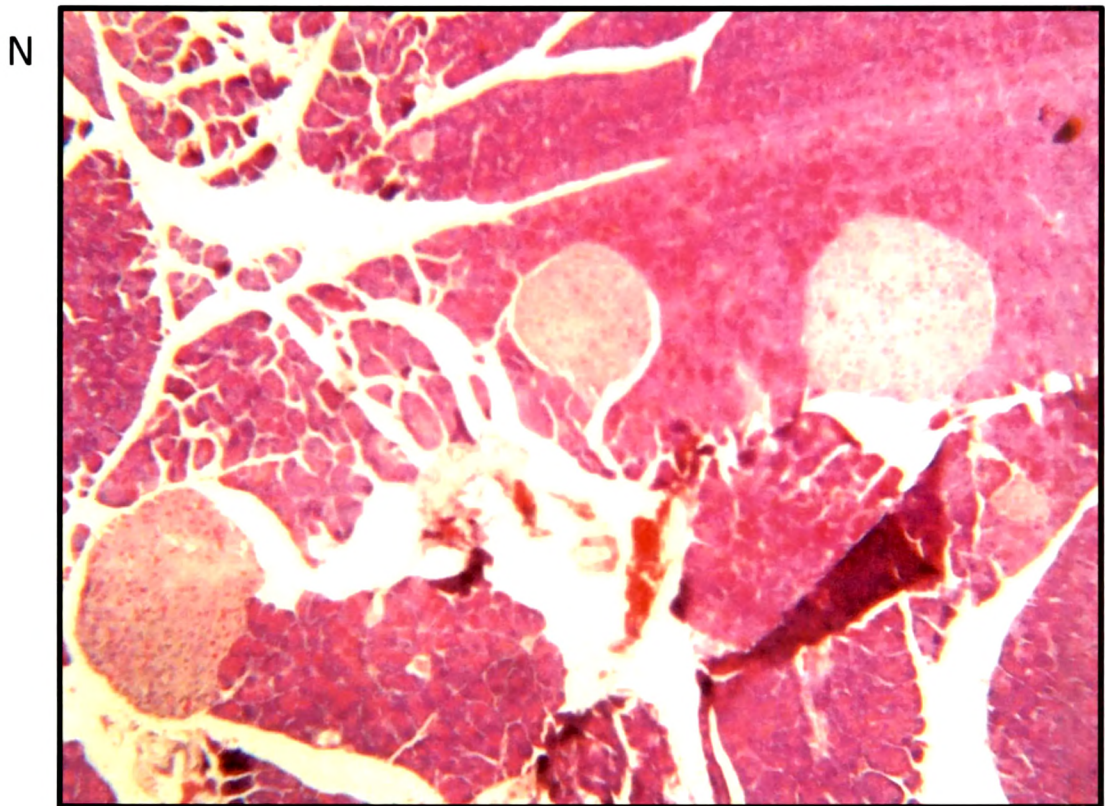
Px day 21

Fig. 3 HAEMATOXYLIN AND EOSIN STAINING OF PANCREAS

O

Px day 7 + FRF

P

Px day 7 + FRF

329
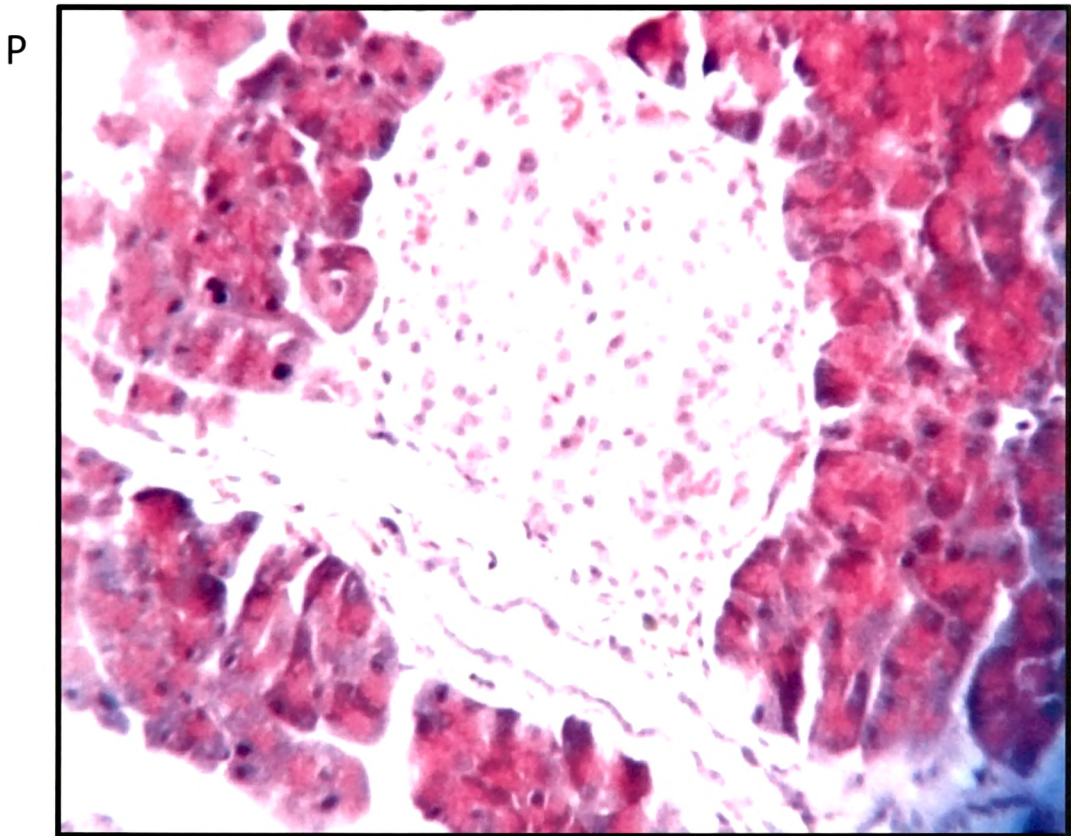
Fig. 3 (O – T): H&E stained sections of pancreas 7 days post Px supplemented with FRF. Note the large number of well formed duct associated prominent looking islet buds with compactly packed cells indicating greater cell proliferation (O, P, S, T: 450 x; Q, R: 100 x).

Fig. 3 HAEMATOXYLIN AND EOSIN STAINING OF PANCREAS
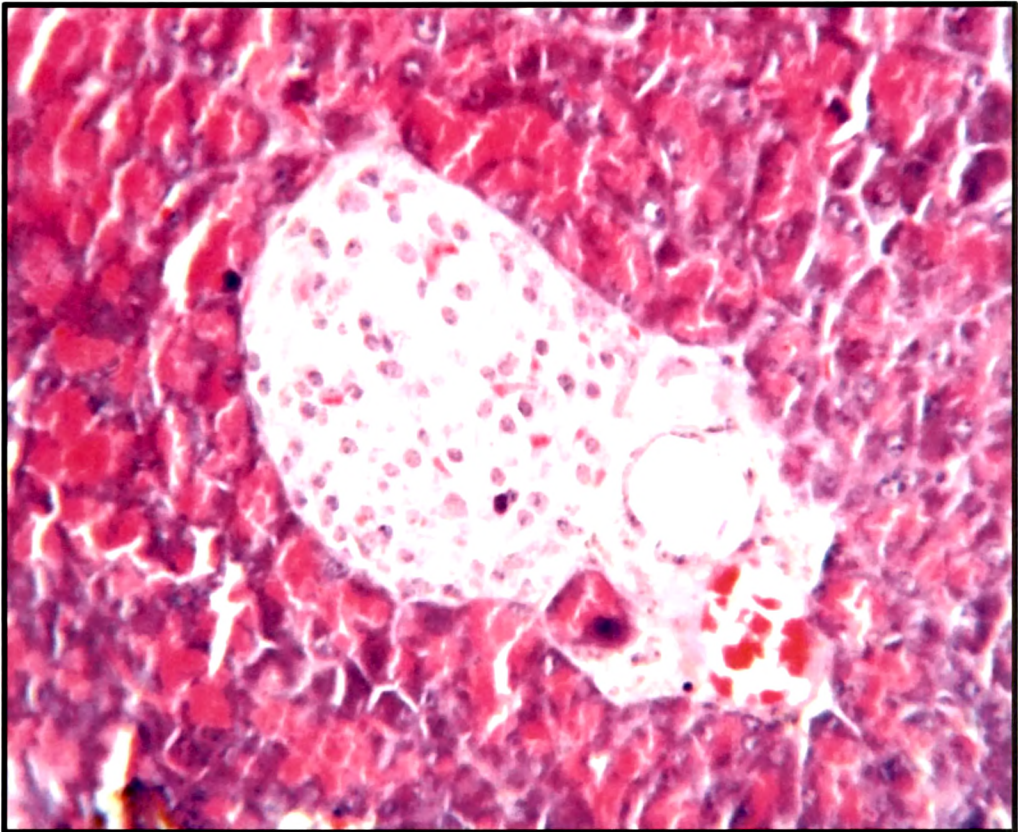
Q

Px day 7 + FRF

R
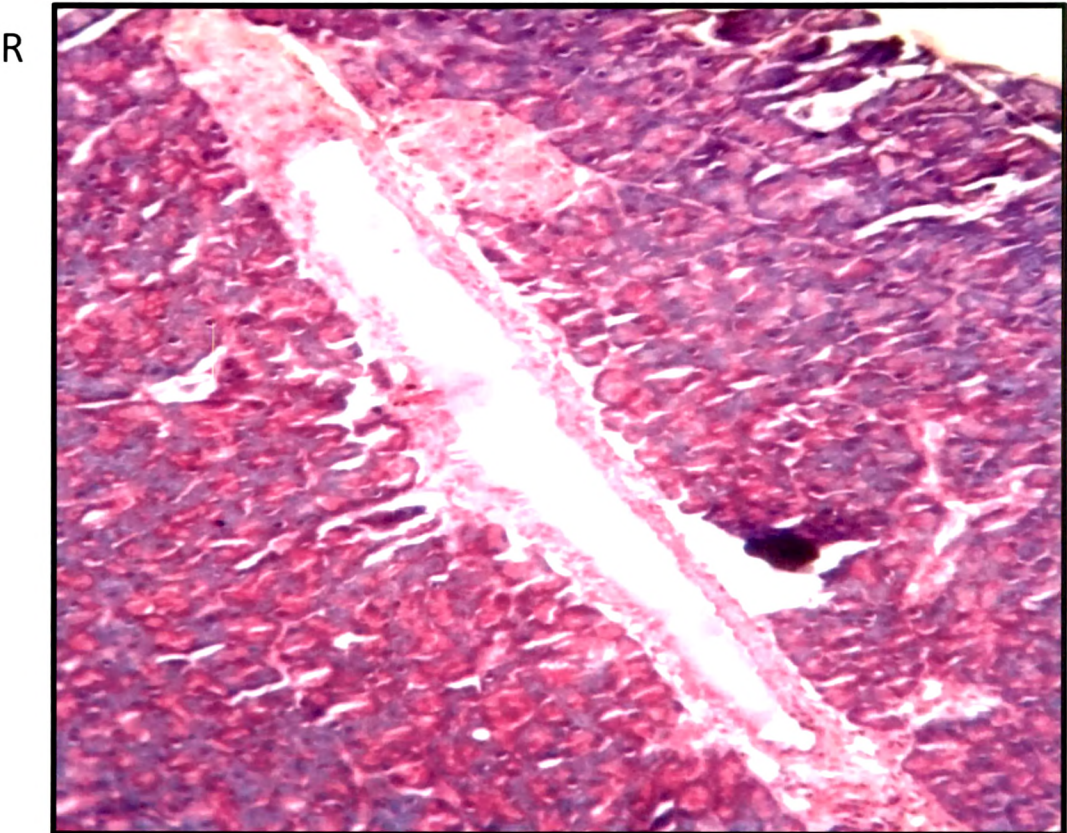
Px day 7 + FRF

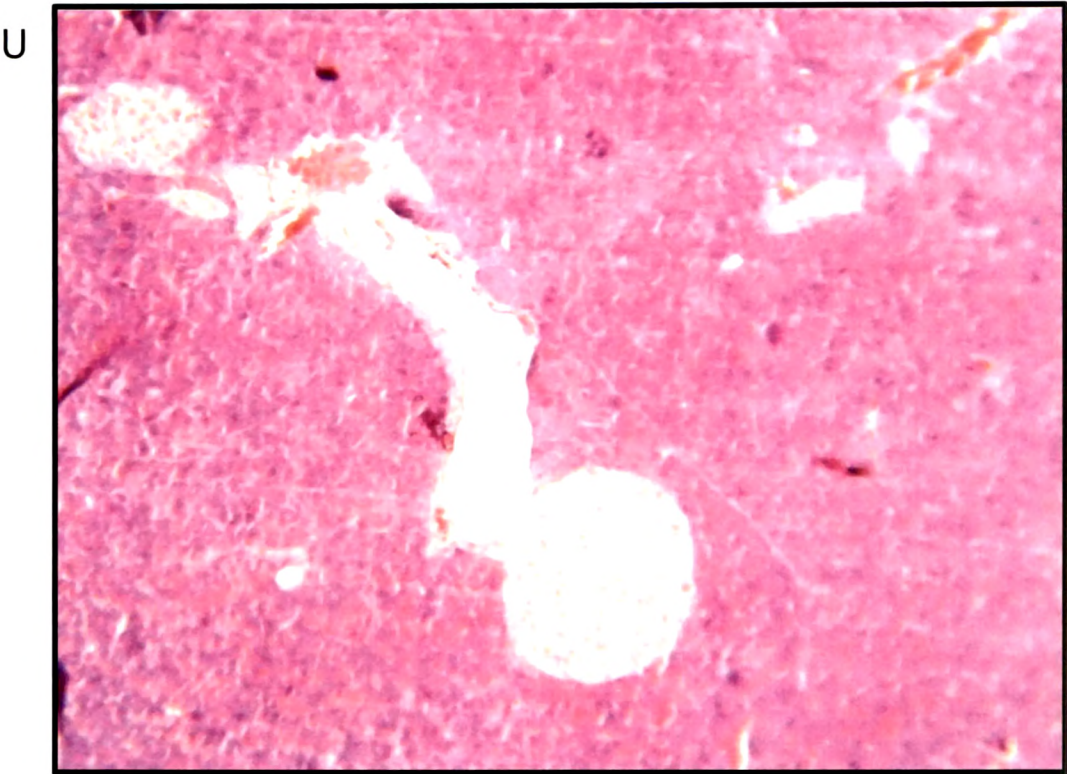# Fig. 3 HAEMATOXYLIN AND EOSIN STAINING OF PANCREAS
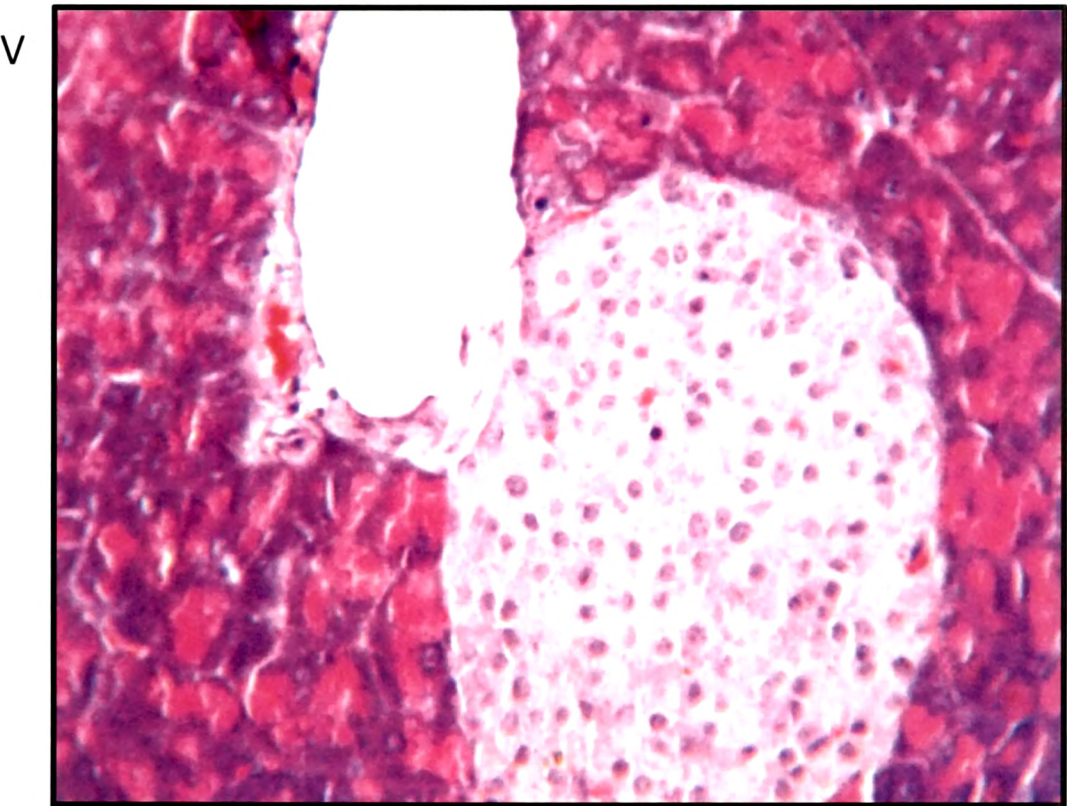
S

Px day 7 + FRF

T

Px day 7 + FRF

Fig. 3 (U – Z): Sections of pancreas of FRF supplemented mice 14 days post Px. Note the larger sized ducts associated islets with proliferating cells in both ducts and islets (U, W, Z: 100x; V, X, Y: 450 x).

Fig. 3 HAEMATOXYLIN AND EOSIN STAINING OF PANCREAS
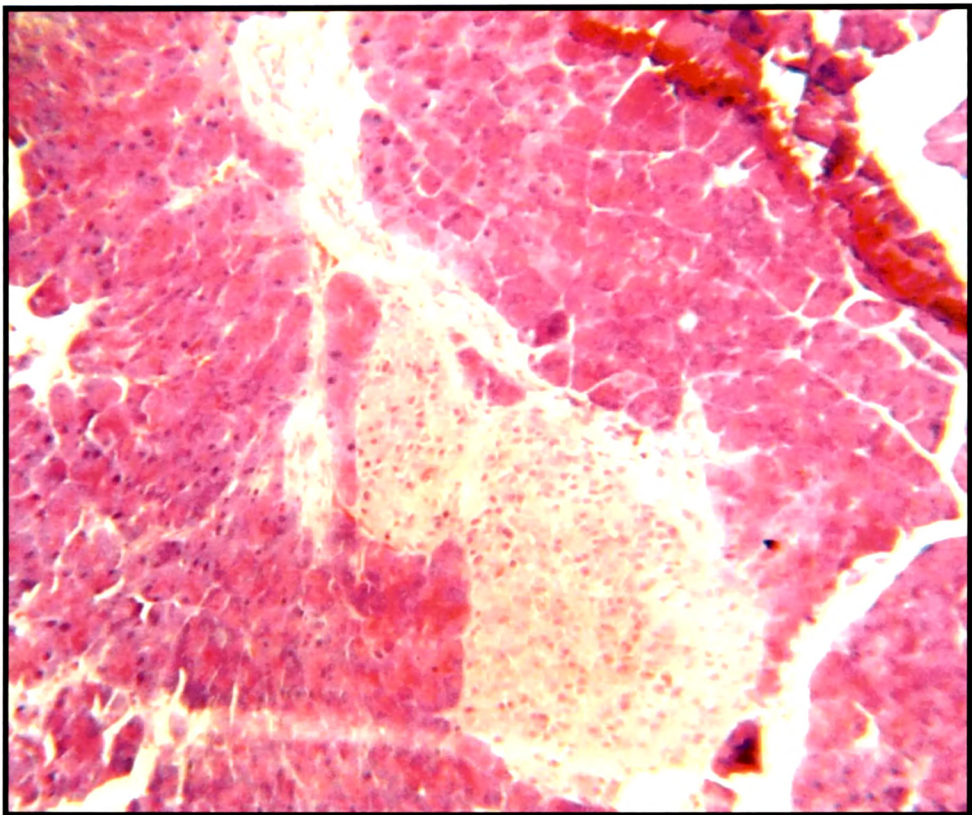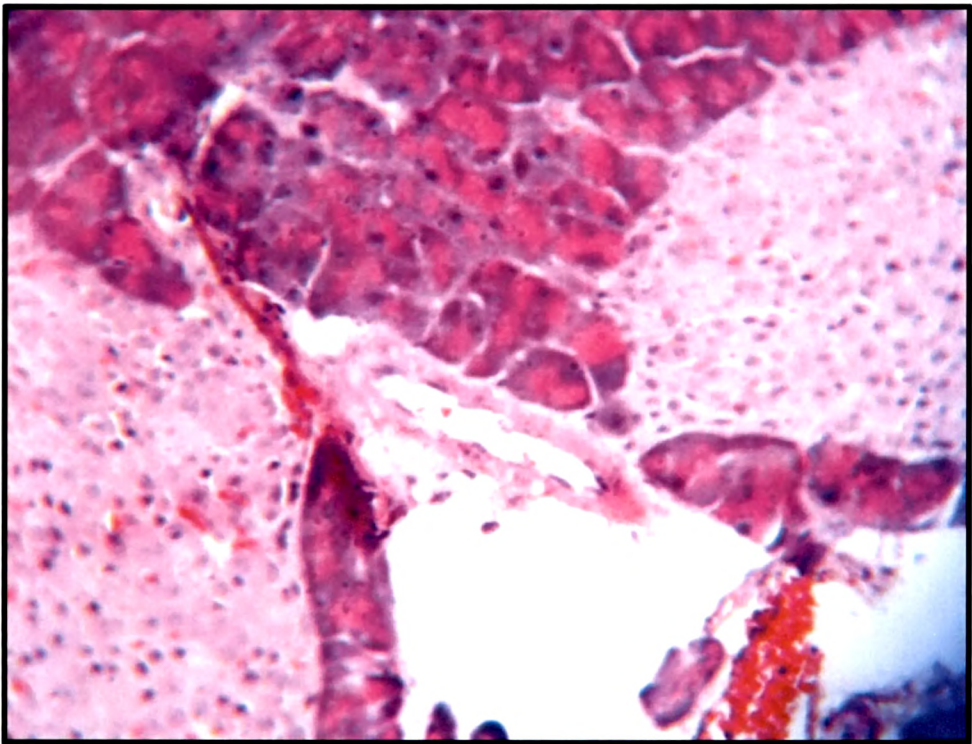
U

Px 14 + FRF

V

Px 14 + FRF

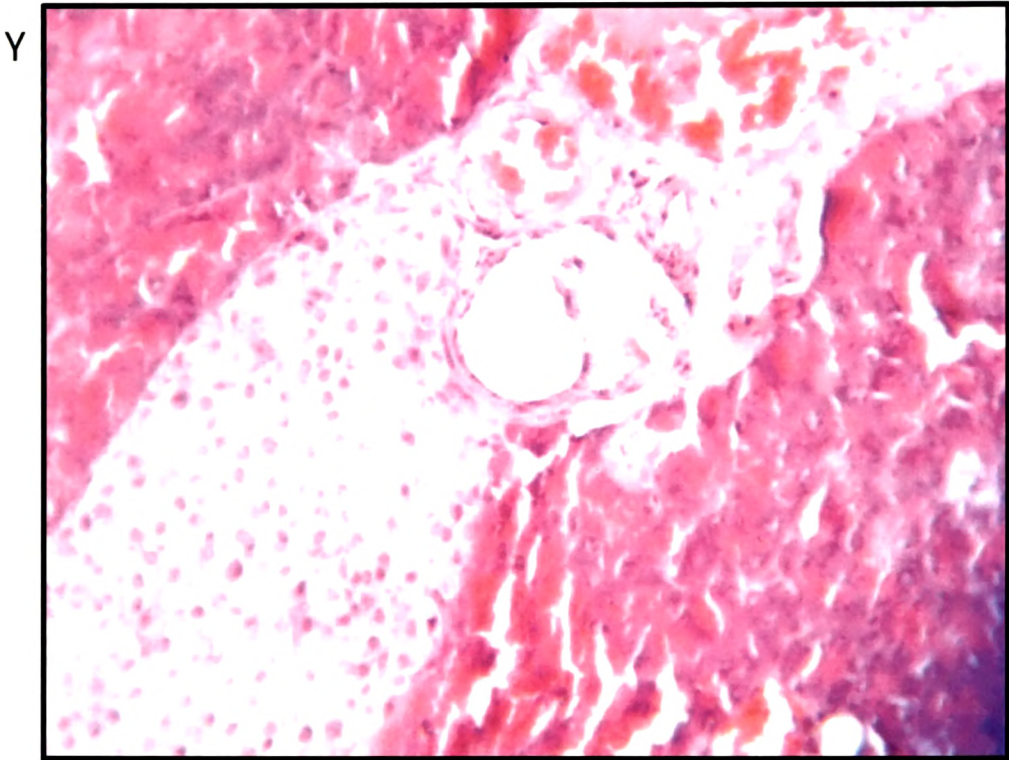# Fig. 3 HAEMATOXYLIN AND EOSIN STAINING OF PANCREAS
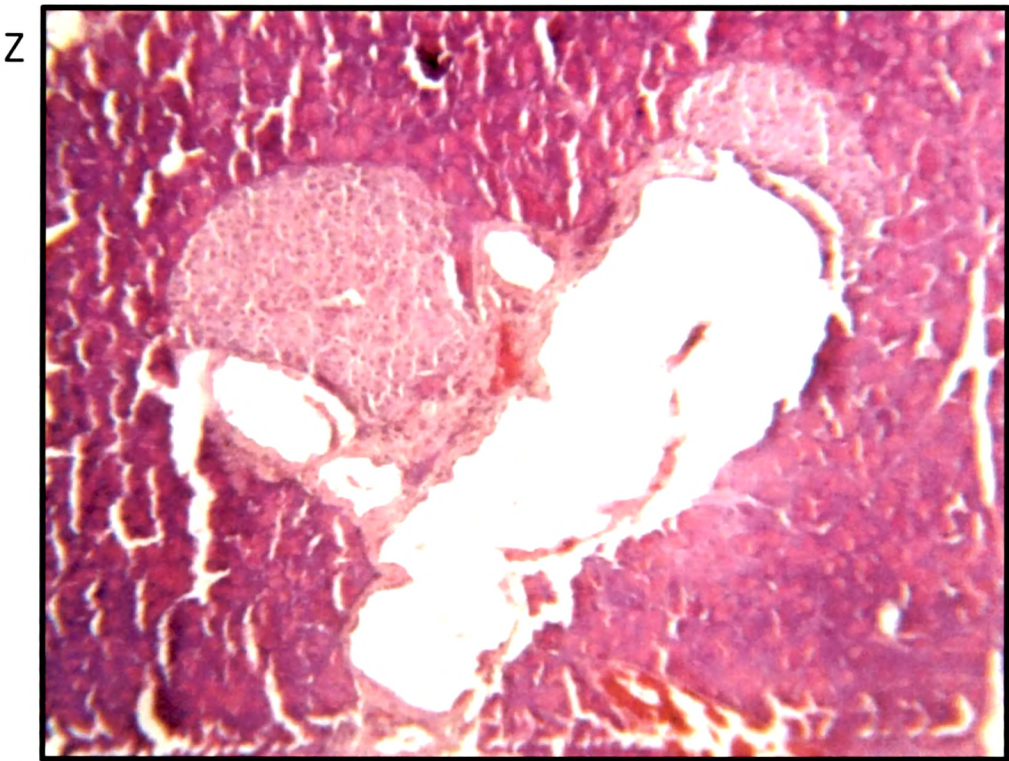
W

Px 14 + FRF

X

Px 14 + FRF

Fig. 3 HAEMATOXYLIN AND EOSIN STAINING OF PANCREAS
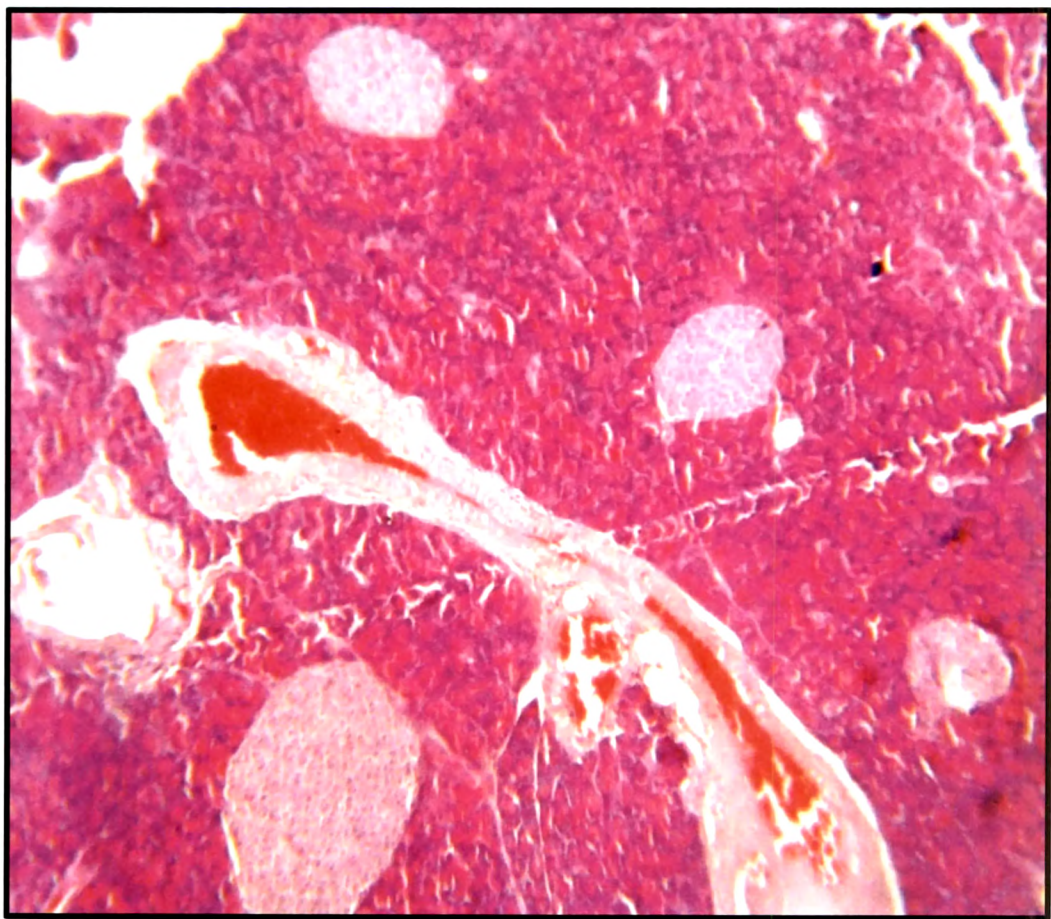

Y

Px 14 + FRF

Z

Px 14 + FRF

Fig. 3 Z 1: Section of FRF supplemented pancreas 21 day post Px. Note the well formed islets within the acini with compactly packed islet cells (100 x).

Fig. 3 HAEMATOXYLIN AND EOSIN STAINING OF PANCREAS

Z 1

Px 21 + FRF

Fig. 4 Images represent immunostained section of pancreas of A) Pancreatectomized mice at day 7 and B) Pancreatectomised mice treated with FRF at day 7. Guinea pig anti insulin (green) and mouse anti BrdU antibody (red) as primaries and Donkey anti GP IgG alexaflour 488 & Donkey anti mouse IgG texas Red as secondaries. Dapi was used to visualize nuclei. Optical slices were taken at ~ 0.8µm.Laser gains, pin hole setting and magnification were set identical across samples. Scale bar represents 50 µm.
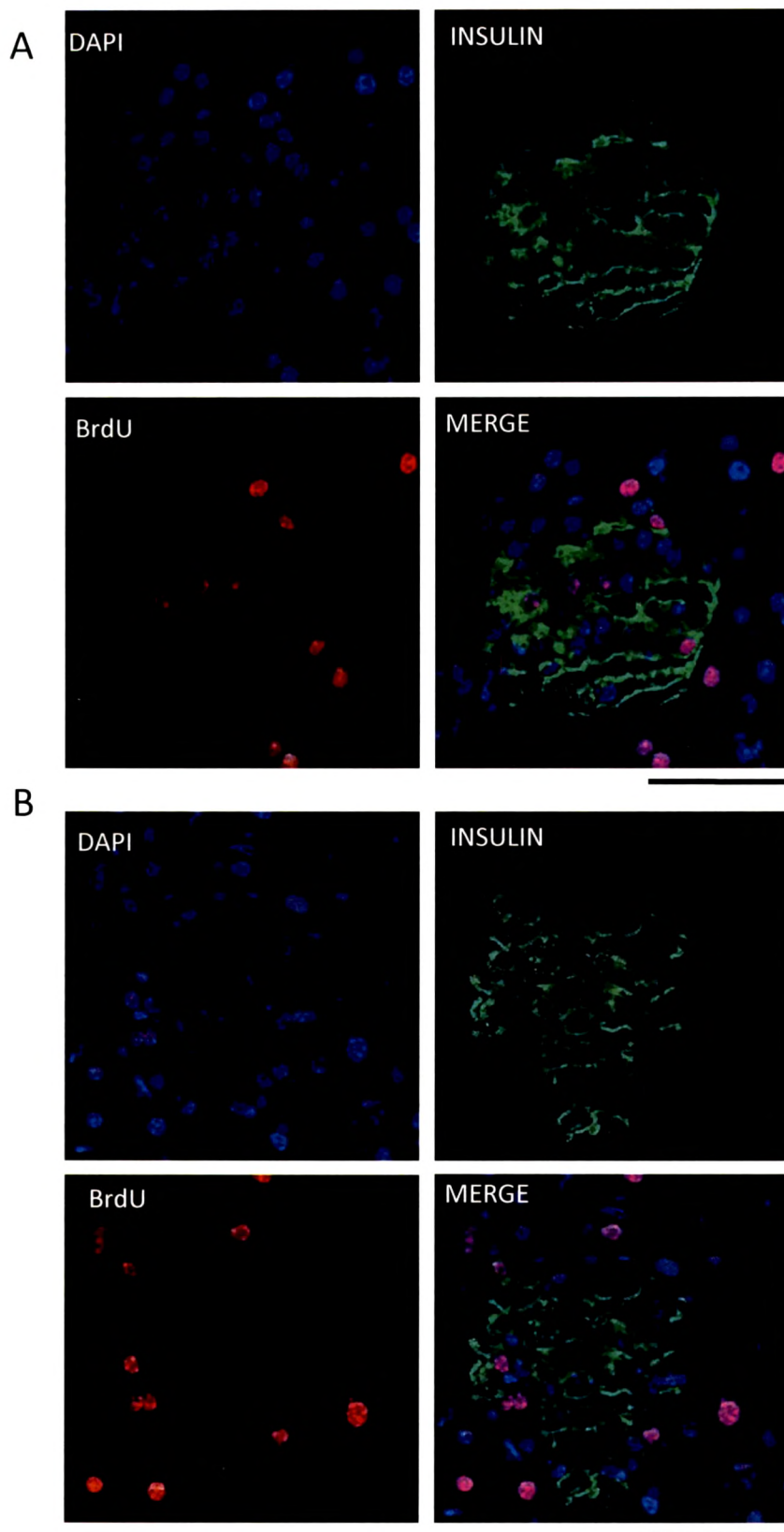
Fig. 5 Images represent immunostained section of pancreas of A) Pancreatectomized mice at day 14 and B) Pancreatectomised mice treated with FRF at day 14. Guinea pig anti insulin (green) and mouse anti BrdU antibody (red) as primaries and Donkey anti GP IgG alexaflour 488 & Donkey anti mouse IgG texas Red as secondaries. Dapi was used to visualize nuclei. Scale bar represents 50 μm.
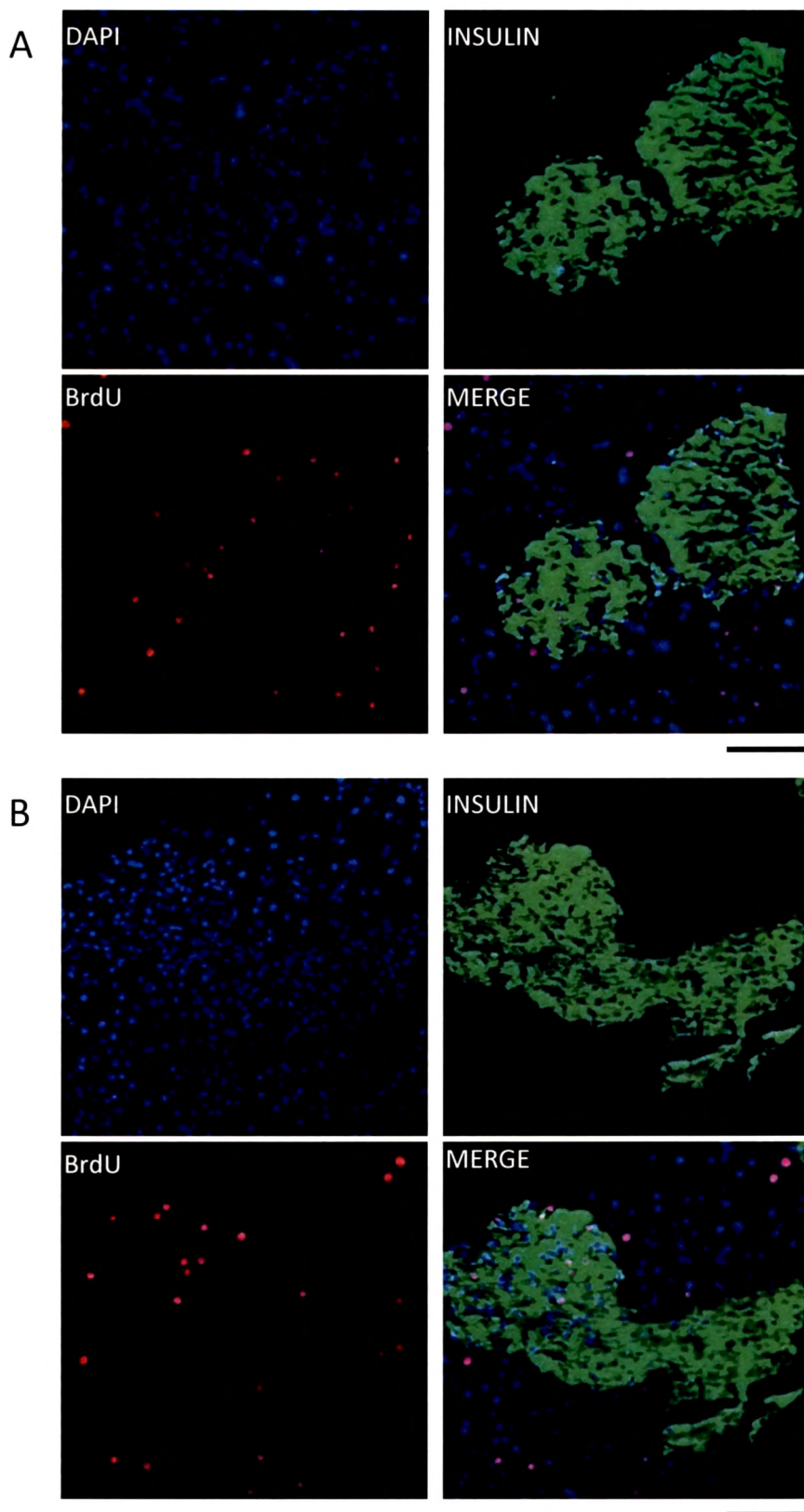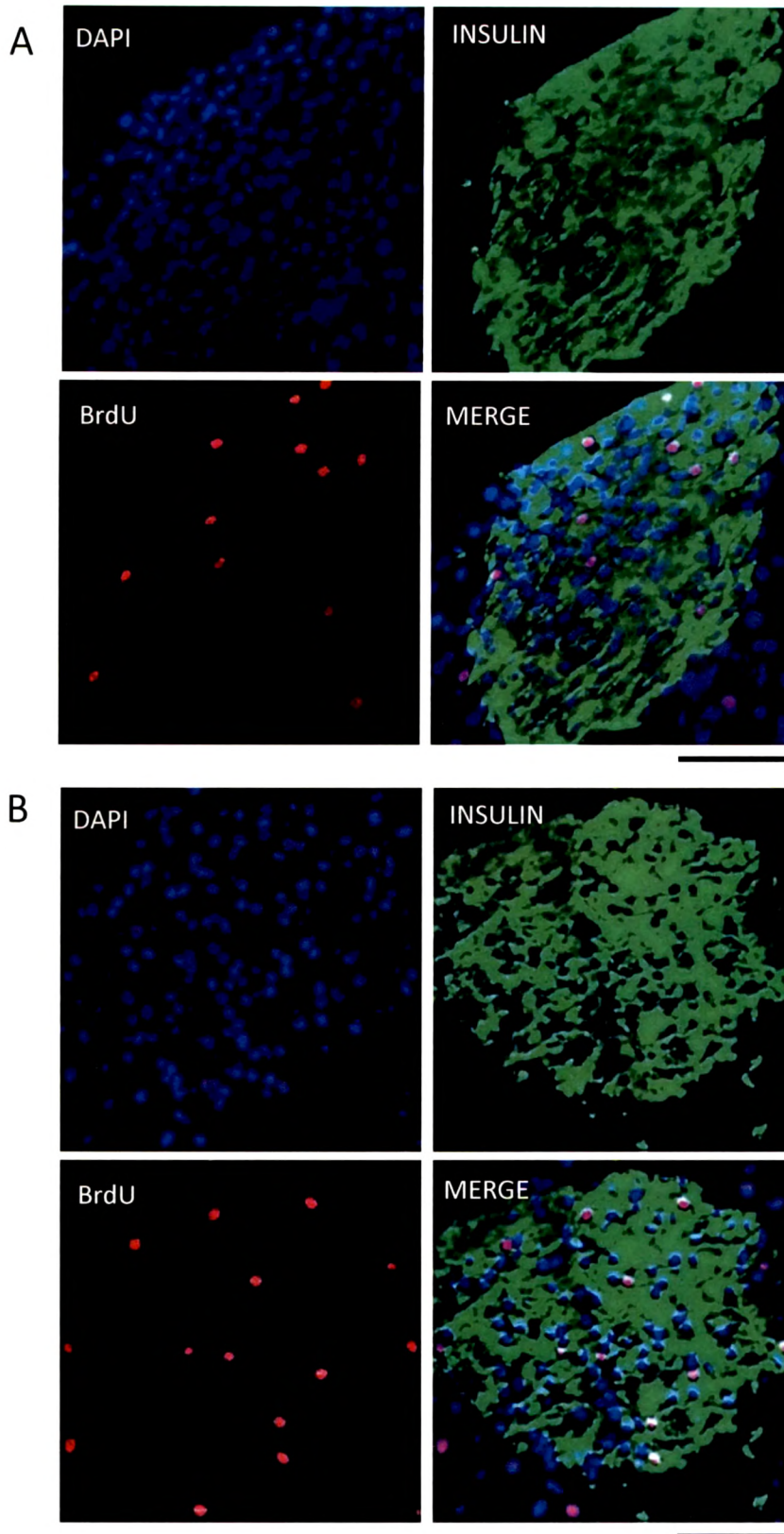
Fig. 6 Images represent immunostained section of pancreas of A) Pancreatectomized mice at day 21 and B) Pancreatectomised mice treated with FRF at day 21. . Guinea pig anti insulin (green) and mouse anti BrdU antibody (red) as primaries and Donkey anti GP IgG alexaflour 488 & Donkey anti mouse IgG texas Red as secondaries. Dapi was used to visualize nuclei. Scale bar represents 50 μm.

338
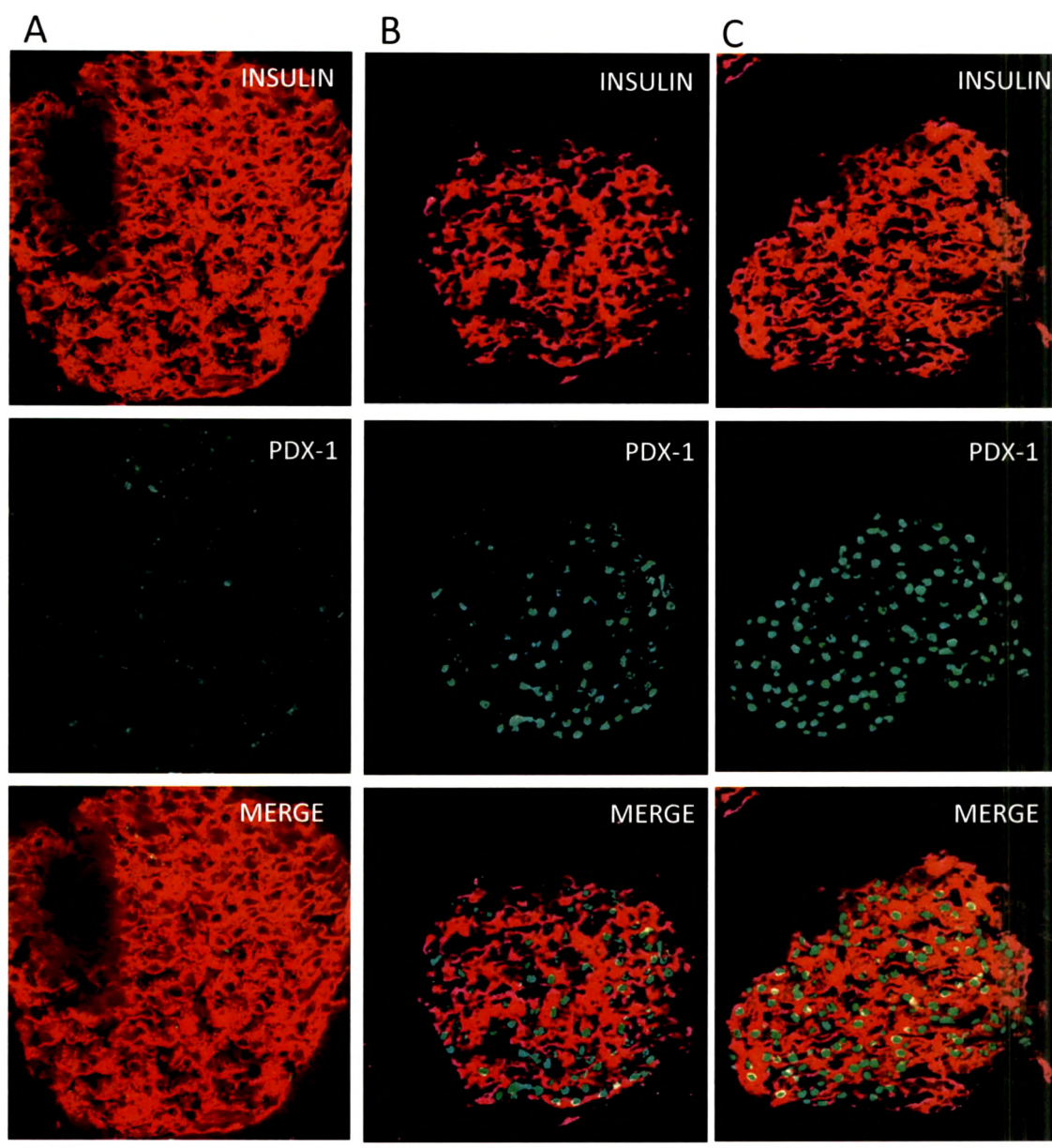
Fig. 7 Images represent immunostained section of pancreas of A) Sham operated mice, B) Pancreatectomized mice at day 7 and C) Pancreatectomised mice treated with FRF at day 7. Guinea pig anti insulin (red) and Rabbit Pdx-1 antibody (green) as primaries and Donkey anti GP IgG alexaflour 594 & Donkey anti rabbit IgG alexaflour 488 as secondaries. Dapi was used to visualize nuclei. Scale bar represents 50 µm.

Fig . 8 BrdU incorporation in islets at different time periods post px
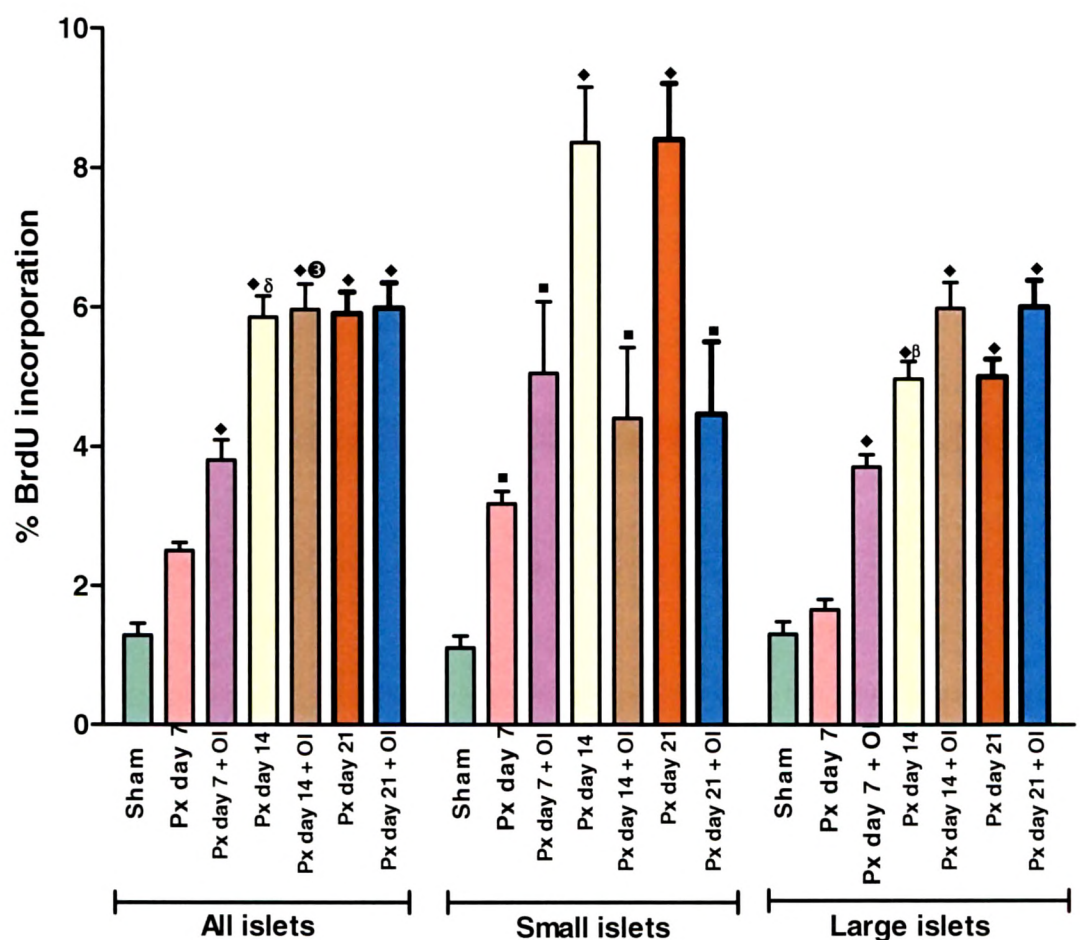
• = p < 0.01, ■ =p <0.001, ◆ =p < 0.0001: Expreimental groups w ere compared to sham

α = p <0.01, β = p <0.001, δ = p <0.0001: px day 7 w as compared to Px day 7 + OI

❸ =p<0.0001: Px day 14 w as compared to Px day 14 + OI

①=p<0.01,②=p<0.001,③=p<0.0001: Px day 21 w as compared to Px day 21 + OI

BrdU incorporation in non-islet cells post day 7 Px

Fig. 9 Representative Image of immunostained section of pancreas depicting BrdU incorporation in non-islet cells of pancreatectimzed mice after day 7. Rabbit glucagon (green) and Mouse BrdU (red) were used as primary antibodies while Donkey-anti-rabbit-IgG-FITC and donkey anti mouse IgG Texas red as secondaries. DAPI (Blue) was used to visualize nuclei. The slides were visualized by Laser Scanning Confocal Microscope (LSM 510 META, ZEISS, Germany).Optical slices were taken at ~ 0.8µm.Laser gains, pin hole setting and magnification were set identical across samples. Scale bar represents 50 µm.

BrdU incorporation in acini post day 7 Px

acini

Fig. 10 Representative Image of immunostained section of pancreas depicting BrdU incorporation in acinar region of pancreatectimzed mice after day 7. Mouse BrdU (red) were used as primary antibody while Donkey anti mouse IgG texas Red as secondary. DAPI (Blue) was used to visualize nuclei. The slides were visualized by Laser Scanning Confocal Microscope (LSM 510 META, ZEISS, Germany).Optical slices were taken at ~ 0.8μm.Laser gains, pin hole setting and magnification were set identical across samples. Scale bar represents 50 μm.

BrdU incorporation in ducts post day 7 Px

• = p < 0.01, ■=p <0.001, ◆=p < 0.0001:control was compared to other experimental groups
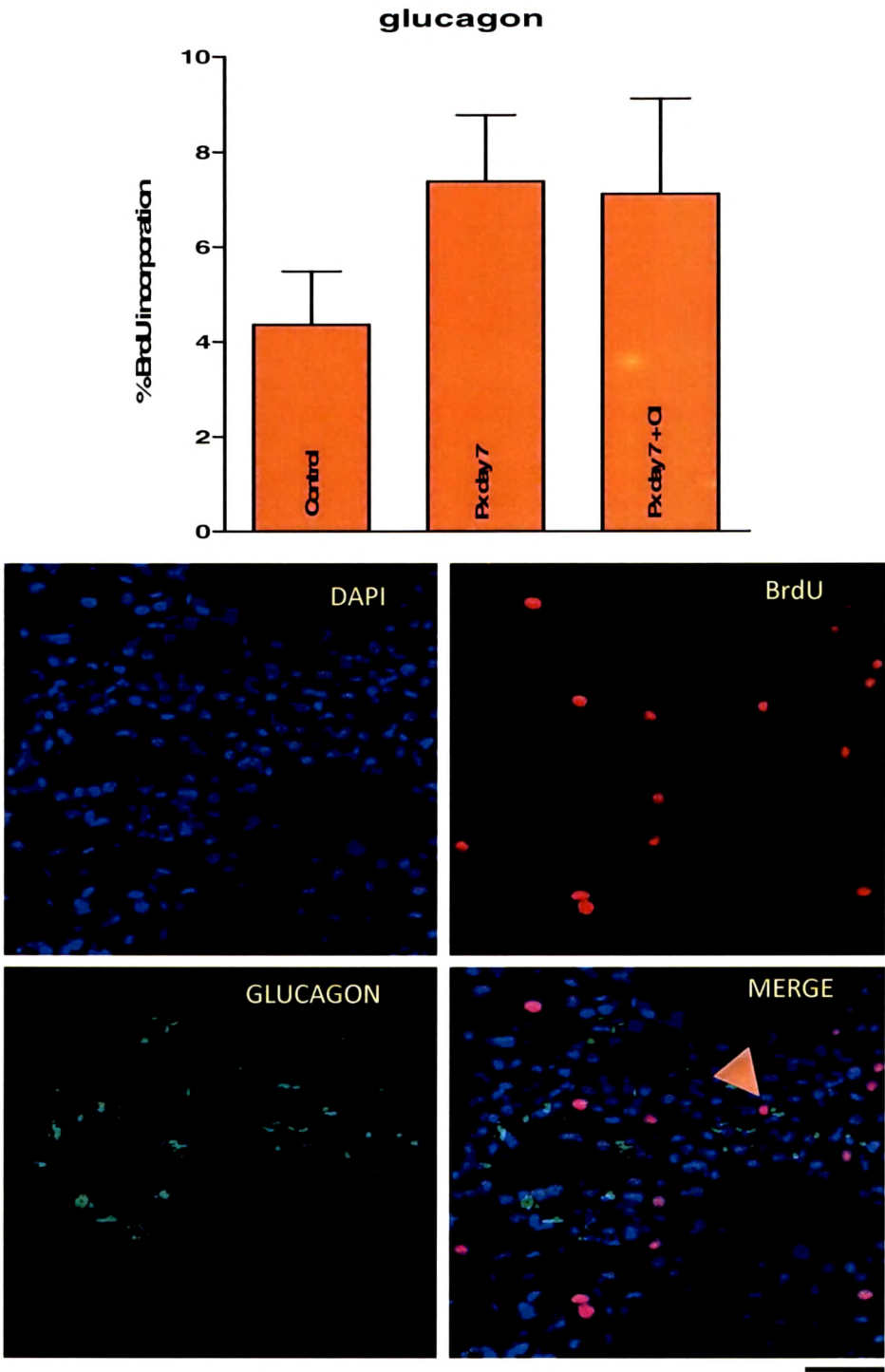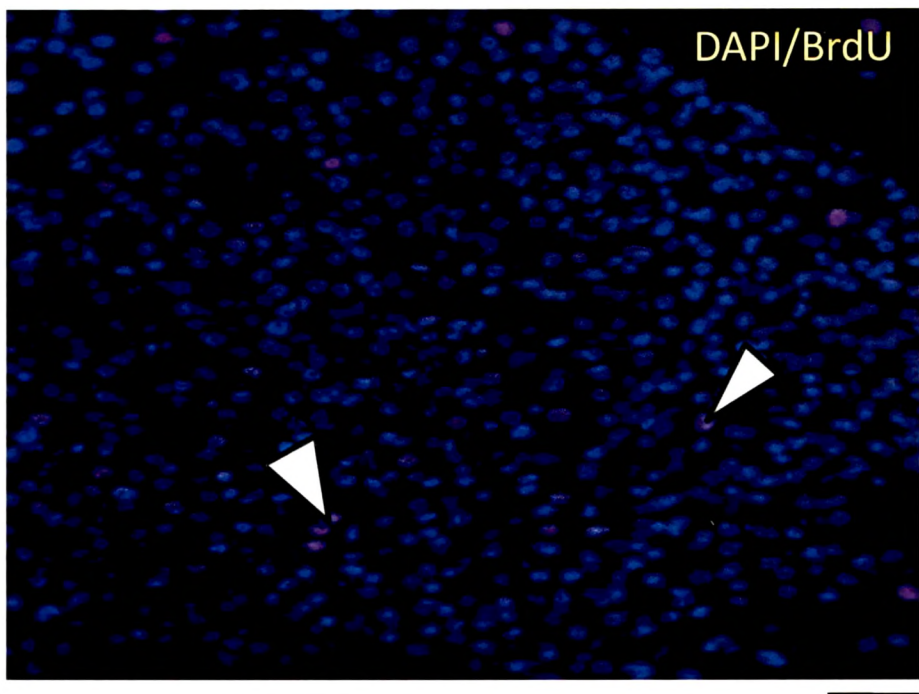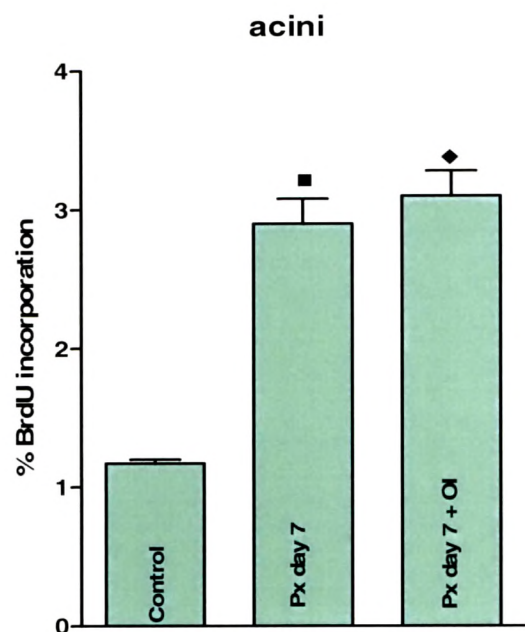α = p <0.01, β = p <0.001, δ = p <0.0001: px day 7 was compared to Px day 7 + OI
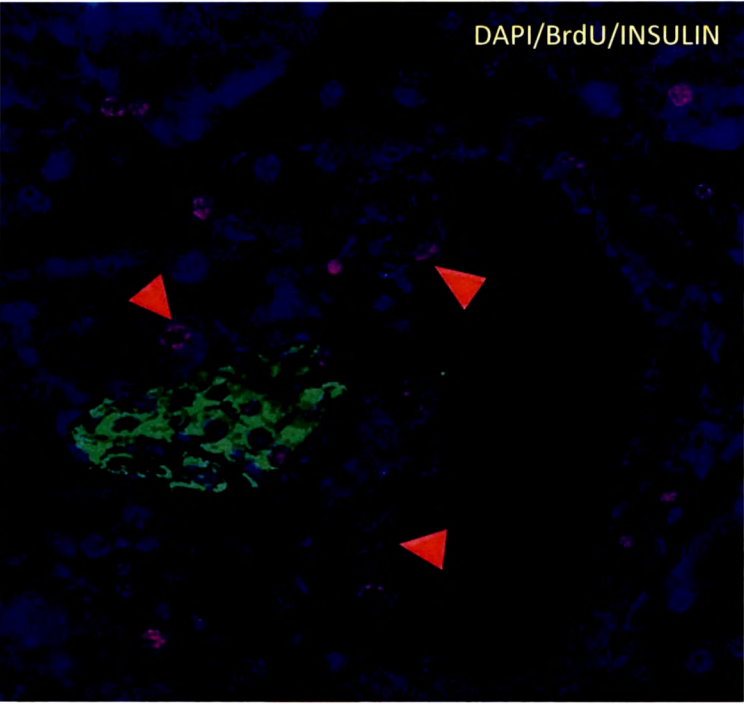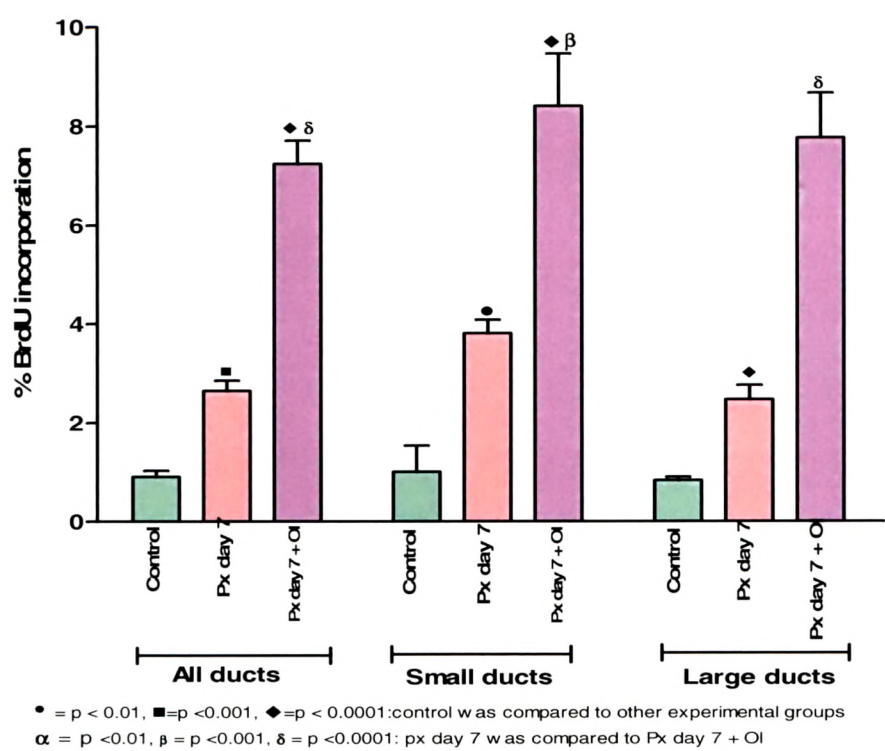
Fig. 11 Representative Image of immunostained section of pancreas depicting BrdU incorporation in duct region of pancreatectimzed mice after day 7 Guinea pig anti insulin (green) and mouse anti BrdU antibody (red) as primaries and Donkey anti GP IgG alexaflour 488 & Donkey anti mouse IgG texas Red as secondaries. DAPI (Blue) was used to visualize nuclei. The slides were visualized by Laser Scanning Confocal Microscope (LSM 510 META, ZEISS, Germany).Optical slices were taken at ~ 0.8μm.Laser gains, pin hole setting and magnification were set identical across samples. Scale bar represents 50 μm.

343

Fig : 12 Effect of FRF on Ins 1 transcripts and their Ct values in Px mice assessed using quantitative pcr
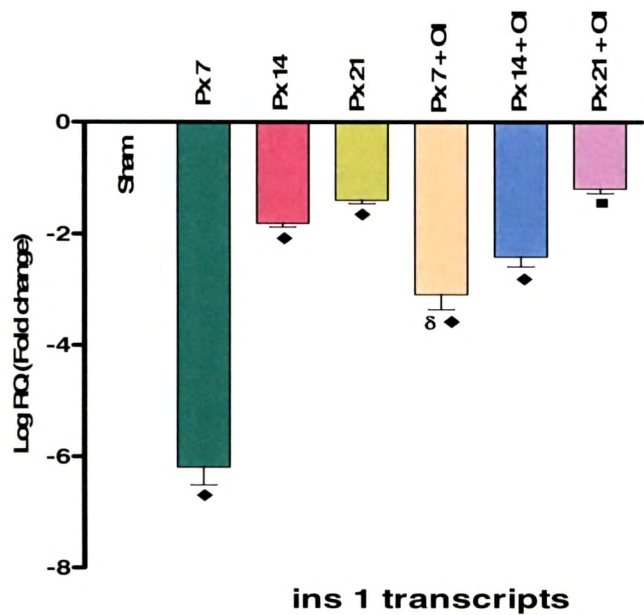
ins 1 transcripts

● = p < 0.05, ■=p <0.01, ◆=p < 0.001:sham was compared to other experimental groups
α = p <0.05, β = p <0.01, δ = p <0.001: Px 7 was compared to Px 7 + OI
❶ = p <0.05, ❷ = p <0.01, ❸= p <0.001: Px 7 was compared to Px 7 + OI

Fig. : 13 Effect of FRF on Ins 2 transcripts and their Ct values in Px mice assessed using quantitative pcr

ins 2 transcripts

● = p < 0.05, ■ =p <0.01, ◆ =p < 0.001:sham was compared to other experimental groups
α = p <0.05, β = p <0.01, δ = p <0.001: Px 7 was compared to Px 7 + OI
❶ = p <0.05, ❷ = p <0.01, ❸ = p <0.001: Px 7 was compared to Px 7 + OI

Fig : 14 Effect of FRF on Reg-3a transcripts and their Ct values in Px mice assessed using quantitative pcr

Reg 3a transcripts

● = p < 0.05, ■=p <0.01, ◆=p < 0.001:sham was compared to other experimental groups

α = p <0.05, β = p <0.01, δ = p <0.001: Px 7 was compared to Px 7 + OI

❶ = p <0.05, ❷ = p <0.01, ❸= p <0.001: Px 7 was compared to Px 7 + OI

Fig : 15 Effect of FRF on Reg-3g transcripts and their Ct values in Px mice assessed using quantitative pcr

Reg 3g transcripts

● = p < 0.05, ■ =p <0.01, ◆ =p < 0.001:sham was compared to other experimental groups
α = p <0.05, β = p <0.01, δ = p <0.001: Px 7 was compared to Px 7 + OI
❶ = p <0.05, ❷ = p <0.01, ❸ = p <0.001: Px 7 was compared to Px 7 + OI

Fig : 16 Effect of FRF on PDX-1 transcripts and their Ct values in Px mice assessed using quantitative pcr

PDX 1 transcripts

● = p < 0.05, ■=p <0.01, ◆=p < 0.001:sham was compared to other experimental groups
α = p <0.05, β = p <0.01, δ = p <0.001: Px 7 was compared to Px 7 + OI
❶ = p <0.05, ❷ = p <0.01, ❸= p <0.001: Px 7 was compared to Px 7 + OI
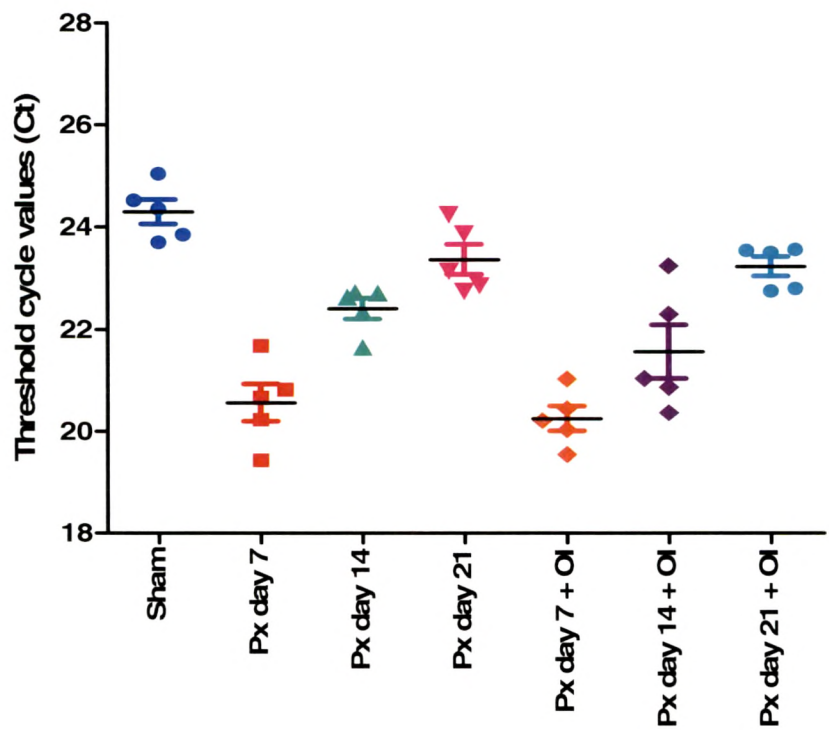
Fig : 17 Effect of FRF on NgN-3 transcripts and their Ct values in Px mice assessed using quantitative pcr

NgN 3 transcripts

● = p < 0.05, ■=p <0.01, ◆=p < 0.001:sham was compared to other experimental groups
α = p <0.05, β = p <0.01, δ = p <0.001: Px 7 was compared to Px 7 + OI
❶ = p <0.05, ❷ = p <0.01, ❸= p <0.001: Px 7 was compared to Px 7 + OI

Discussion:

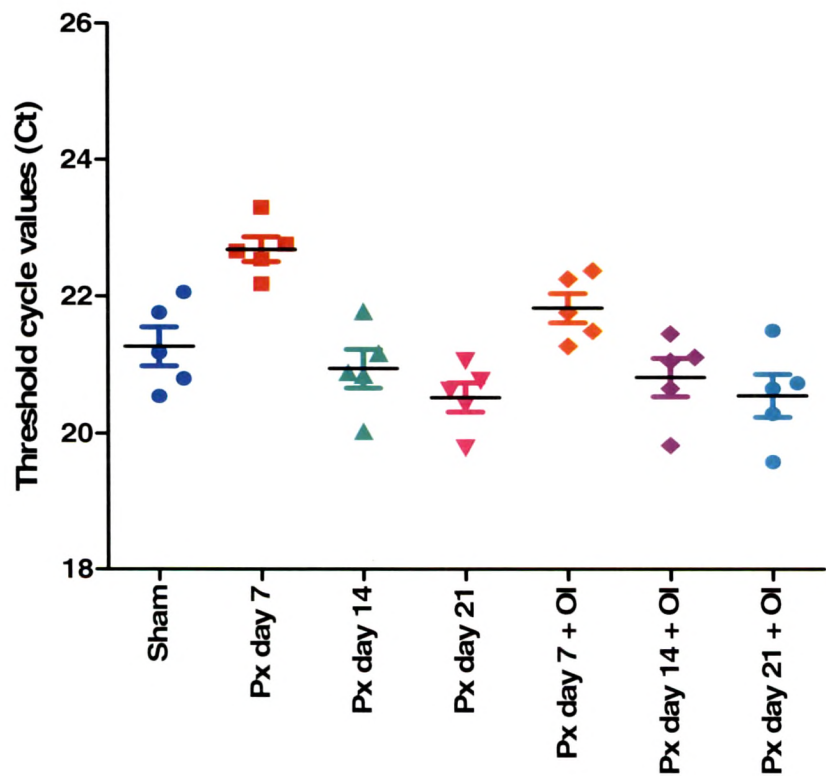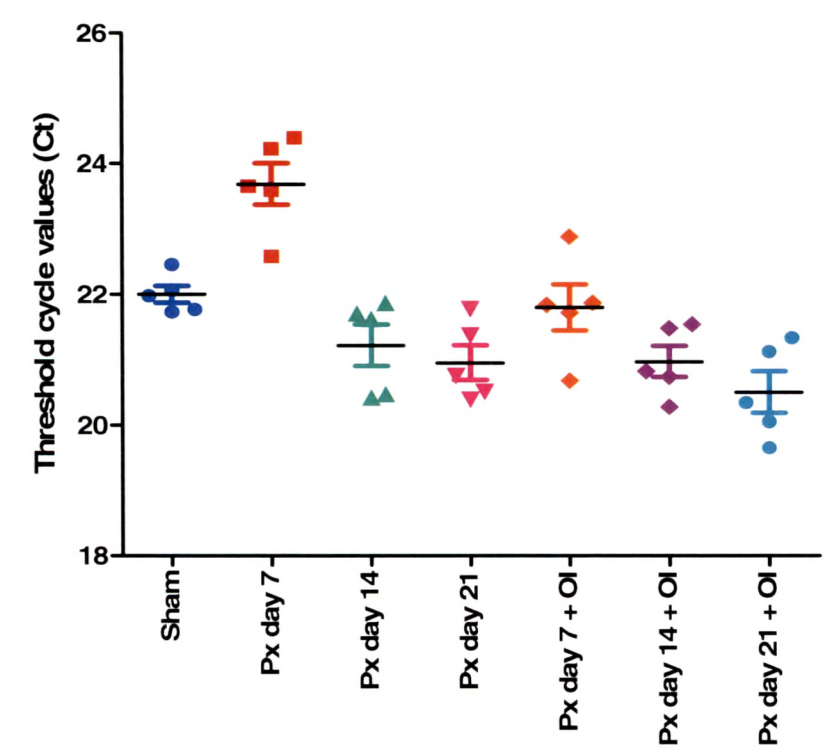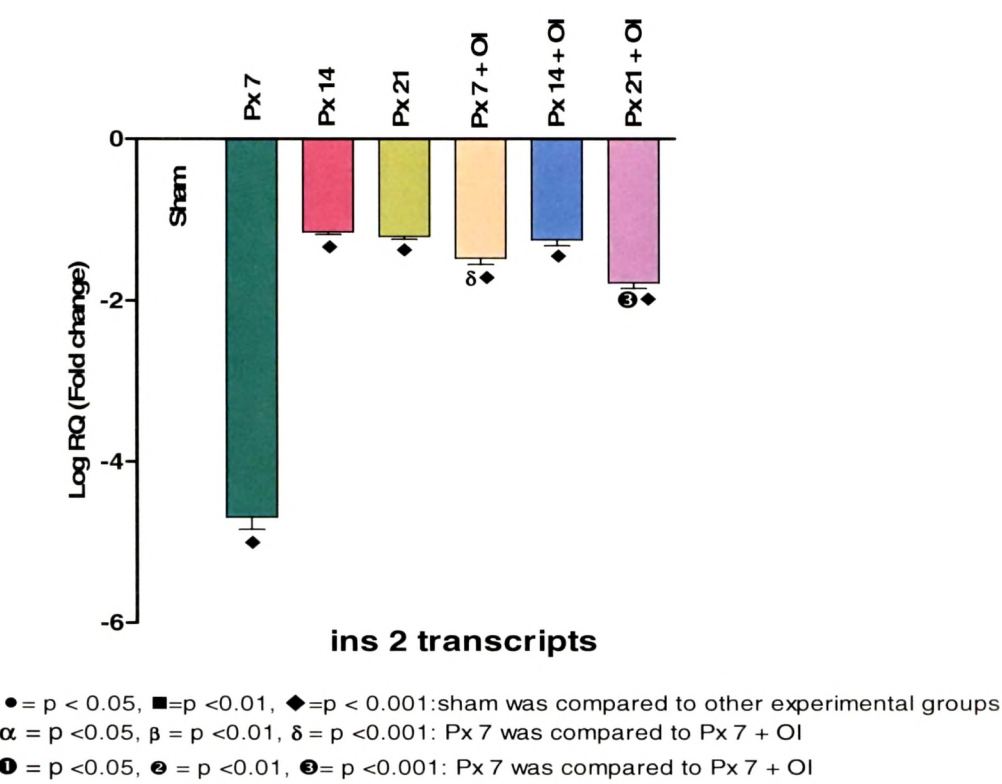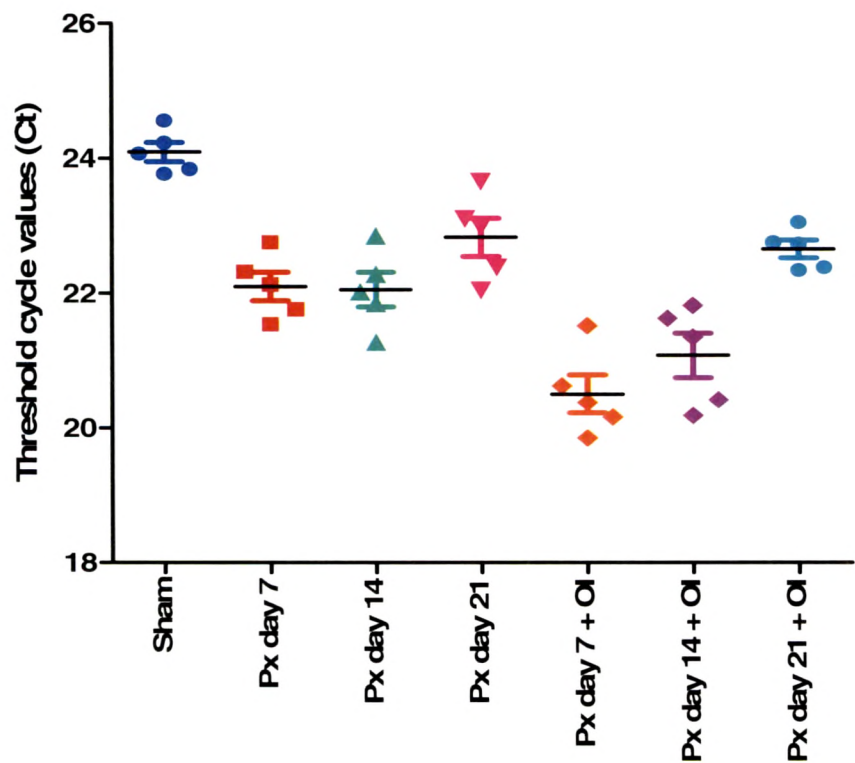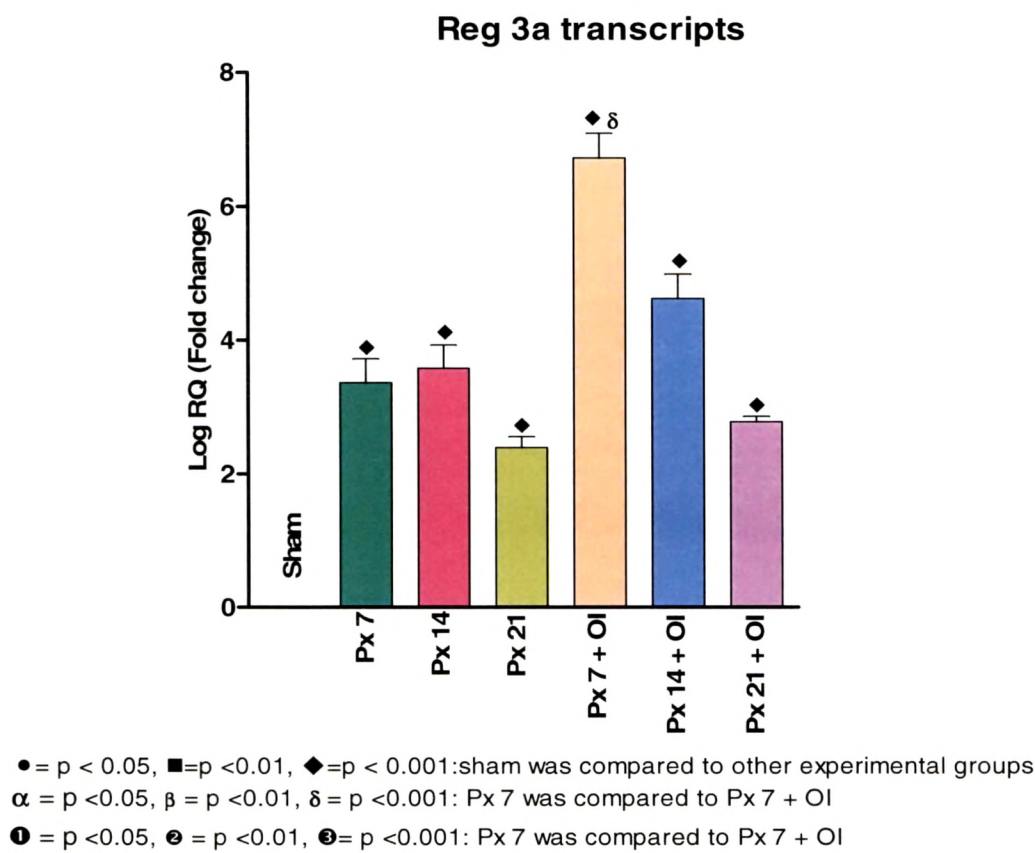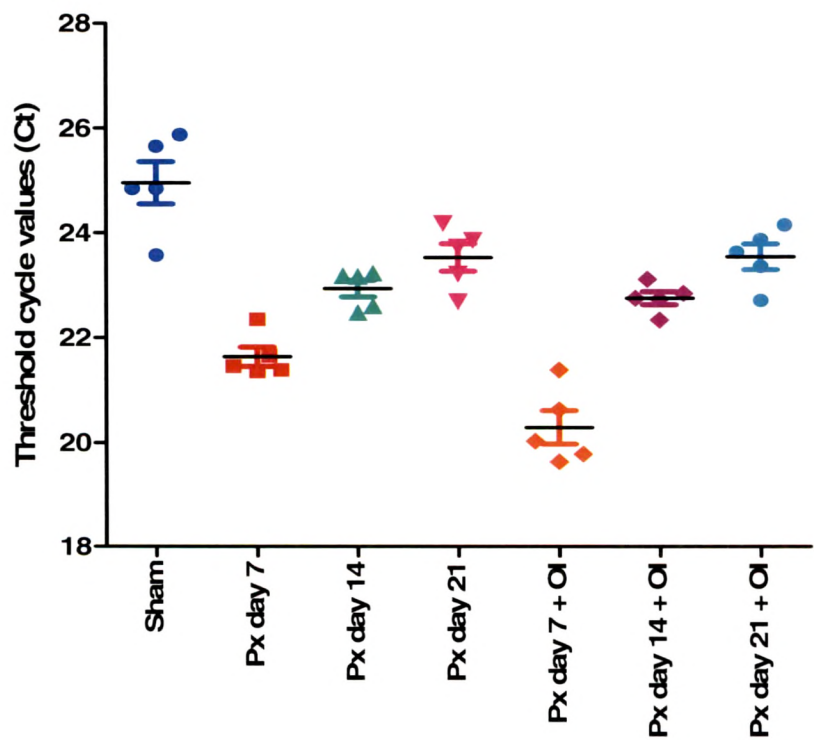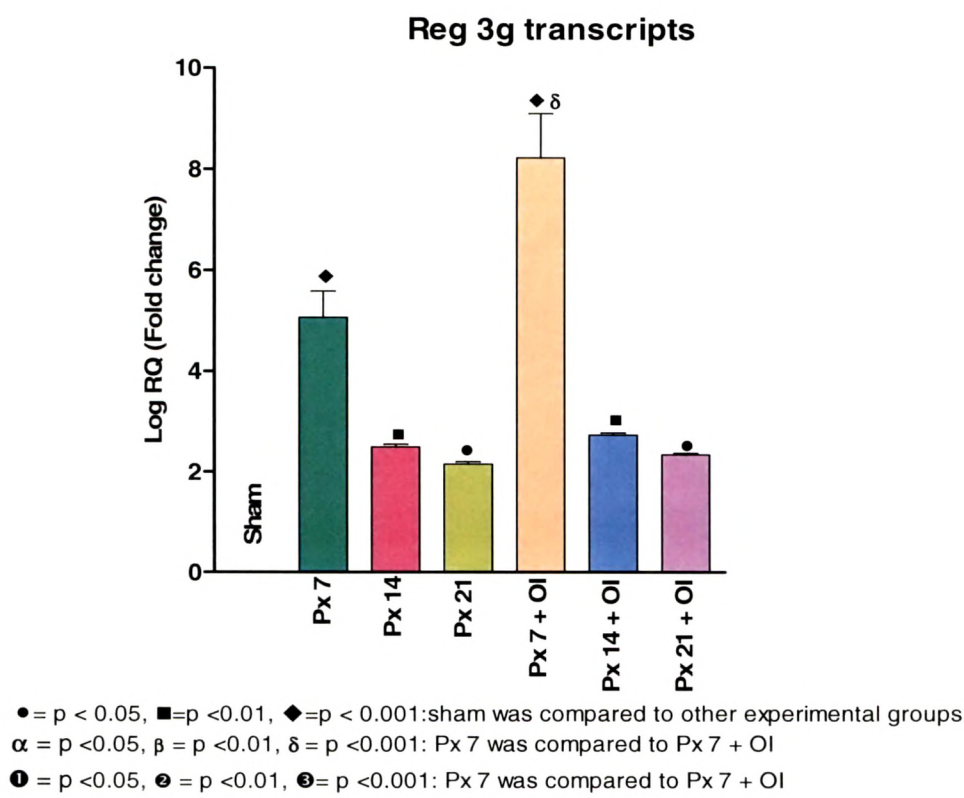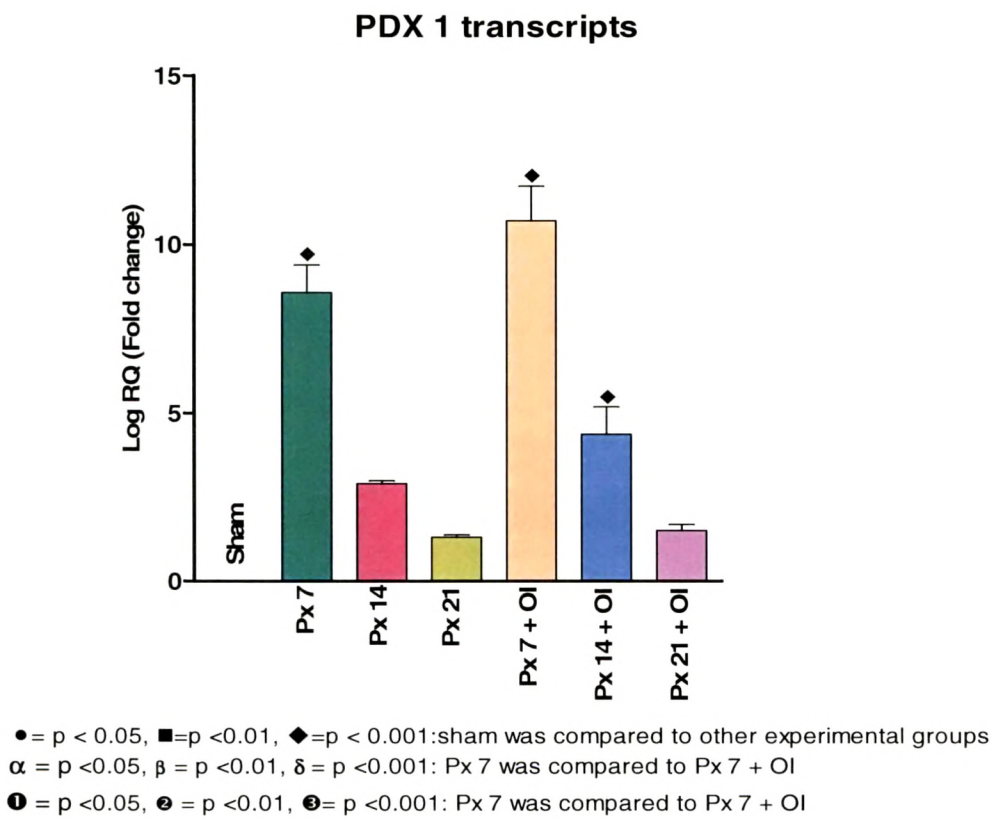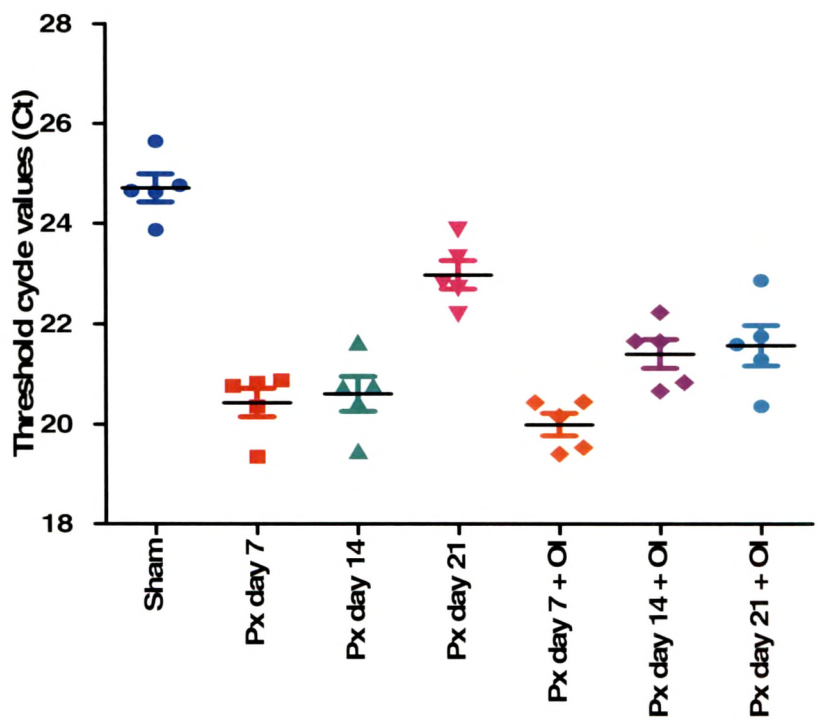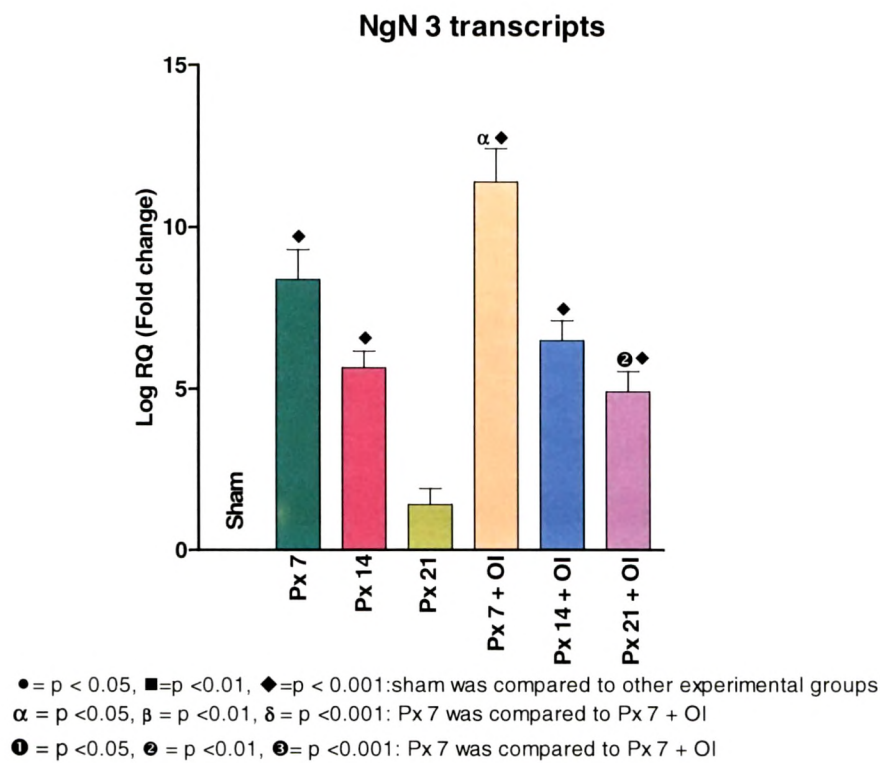The present study on pancreatectomised (70%) BALB/c mice from day 7 to day 21 provide clear histocytochemical evidence for a ductal contribution in islet neogenesis with specific expression of regeneration and proliferation promoting genes. Literature, in recent times, is replete with a spectrum of experimental evidences and contentions supporting differing hypotheses of islet / β-cell formation under a variety of natural and experimental conditions. These studies have tended to suggest widely differing mechanisms like islet / β-cell neogenesis from ductal precursors / stem cells (Gu and Sarvetrick, 1993; Xia et al., 2009; Solar et al., 2009; Xu et al., 2010; Aye et al., 2010), proliferation of differentiated islet β-cells or intra islet precursor β-cells (Guz et al., 2001; Dor et al., 2004; Teta et al., 2005; Lee et al., 2006; Nir et al., 2007), acinar and stellate cells (Mashima et al., 1996a,b ; Gu et al., 1997; Zhon et al., 1999; Larden et al., 2004; Topp et al., 2004; Means et al., 2005) or even both acinar and ductal cells (Haro-Hernandez et al., 2004). Removal of 70% pancreatic mass in BALB/c strain of mouse is clearly marked by a definitive regenerative reconstitution of pancreatic mass by significant islet neogenesis from ductal cells. The histological observations provide compelling evidence for nodular budding of differentiating endocrine cells that get organised as definitive islets by 21 days post Px. Histological observations further provide convincing evidence for quantitatively greater number of neogenic islet nodes and β-cell density in the pancreas of mice treated with flavonoid rich fraction, suggesting the additional stimulatory role of OI extract flavonoids over and above that of the stimulatory trigger provided by the substantial decrement in pancreatic mass. Augmented rates of cell proliferation in ductal precursor cells in Px pancreas and even higher proliferation in Px + FRF are clearly indicative by the recorded higher BrdU incorporation and BrdU

350

labelling indices. The percentage increase in BrdU incorporation seen here provides strong evidence for the greater potential of FRF to augment ductal precursor stem cell proliferation on subtotal pancreatectomy.
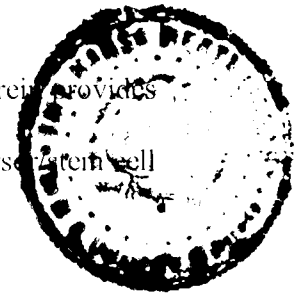
The fact that BrdU incorporation is seen even in presumptive islets associated with ducts also denote continuing proliferation of committed islet cells (β-cells) even after budding off from the ducts. Apparently, islet growth and increase in cell mass could occur by proliferation of immature/ young β-cells. Such intra-islet proliferation of β-cells is documented even in other conditions of β-cell regeneration. Comparatively, proliferation within smaller islets is more intense than in larger islets. Apparently, smaller islets represent newly budded neogenic endocrine cell clusters from the ducts and hence, the tempo of proliferation, initiated within the ducts due to trigger of initiation of pancreatic regeneration, still persists. Though there is a slowing down of the tempo of proliferation within the larger follicles, proliferative increment of β-cell mass nevertheless continues. From available evidence for intra-islet β-cell proliferation, it is presumable that, FoxM1 expression within the committed β-cells subsequent to neogenesis from ductal stem cells and / or transdifferentiation of ductal cells may be of relevance in continued intra-islet β-cell proliferation (Misfeldt *et al.*, 2008; Xu *et al.*, 2010). Though the BrdU incorporation studies also identify acinar cell proliferation during pancreatic restoration post surgery, their contribution to islet morphogenesis is almost nil in the present set up of pancreatic regeneration induced by subtotal pancreatectomy. However, there are some evidences for contribution of acinar cells in islet β-cell formation by transdifferentiation under conditions of neoplastic conversion through EGFR signalling (Means *et al.*, 2005), under *in vitro* conditions (Rooman *et al.*, 2000; Minami *et al.*, 2005; Lipsett *et al.*, 2007). Some studies from our laboratory on neonatal programming by induced melatonin excess or

deficient and adult phenotype plasticity changes have revealed transdifferentiation of acinar cells in the immediate vicinity of islets to β-cells under adult diabetic stress (Adi, 2004; Jani, 2004). Even the current histological observations also hint at the possible participation of few acinar cells in the region of duct derived islets, more so in FRF treated mice. However, it is evident that, islet neogenesis following pancreatectomy principally involves a ductal contribution. The present observations and many other reports contradict the findings of Dor et al. (2004) and Lee et al. (2006) of adult β-cells and not ductal cells as the source of islet regeneration post pancreatectomy. The discrepancies between the two sets of observations need to be closely scrutinised for the strain of animal used, methodology, degree of loss of pancreatic mass etc to find explanation for the apparent contradictory concepts.

It is clear by now that, pancreatic dysfunctioning, like in cases of pancreatectomy, pancreatitis or pancreatic ductal obstruction, is characterised by activation of endogenous stimulators of pancreatic regeneration that may involve soluble autocrine, paracrine and juxtacrinic modulators (Rosenberg, 1998; Hardikar et al., 1999; De Leon, 2003; Kanitkar and Bhonde, 2004). Some of the trophic factor therapies employed for β-cell /islet regeneration are INT, a combination of gastrin and epidermal growth factor (Brand et al., 2002; Saurez-Purizon et al., 2005), glucagon like peptide-1(GLP-1), (De Leon, 2003; Drucker, 2003; Gallwitz, 2006) and INGAP (Rosenberg et al., 2004; Vinick et al., 2004; Pittenger et al., 2007). What stimulus is provided by surgical stress of pancreatectomy or, loss of a critical mass of pancreas, is not clear though, it is clear from the observations that, a powerful inductive regeneration signal is generated. Since, a powerful environmental milieu needs to be created for bringing about islet neogenesis and pancreatic regeneration, generation of a number of initially exclusive and / or inclusive signals can be considered as a

distinct possibility. It is worth contemplating on the possibility of Pdx-1 reduction as one of the possible cues for islet neogenesis in this scenario. Compelling thrust for such a consideration is provided by the fact that, Pdx-1 reduction is a distinct possibility consequent to more than 70% pancreas ablation/loss as, this transcription regulator is expressed in mature β-cells for maintenance of β-cell functions and prevention of glucagon production (Holland *et al.*, 2005) and, Pdx-1 repression is shown to stimulate ductal cell proliferation and upregulate genes known to be associated with islet and β-cell regeneration (Bonner-Weir *et al.*, 1993; Lipsett and Finegood, 2002; Holland *et al.*, 2005). Pdx-1 is an important transcription factor essential initially for early delineation of pancreas from the posterior foregut endodermal analogue (Wilson *et al.*, 2003) and later for maturation of endocrine lineages and β-cell differentiation (Holland *et al.*, 2005; Kodama *et al.*, 2005). Though ductal precursor cell proliferation is triggered by decrease in Pdx-1 and other inducer trophic factors, the ultimate effector molecules appear to be islet neogenesis associated protein (INGAP) and / or other related group-three regeneration promoting proteins (Reg 3), which make the proliferating ductal cells to differentiate, grow into a mass and bud off from the duct to form islet like aggregations (Petropavlovskaia *et al.*, 2006; Lipsett *et al.*, 2007; Taylor-Fishwick *et al.*, 2008). Though a super-family of regeneration promoting proteins, the Reg super-family consisting of Reg-1, Reg-2, Reg-3 isoforms and Reg-4 and IGNAP, are all reported to find expression in pancreas during β-cell regeneration (Rosenberg, 1998; Okamoto, 1999; Qiu *et al.*, 2005; Bluth *et al.*, 2006; De Leon *et al.*, 2006; Lu *et al.*, 2006; Planas *et al.*, 2006; Taylor-Fishwick *et al.*, 2008; Marselli *et al.*, 2010), a careful consideration of these reports reveals the fact that, the expressions of these genes/ proteins are related to the type of pancreatic insult and, further that, Reg-1, Reg-2 and Reg-3β expression are more

353

characteristic of intra-islet β-cell proliferation and regeneration while, Reg-1, Reg-3α and Reg-3γ expressions are more under conditions of islet neogenesis from non-islet sources. In this context, the present study clearly shows higher expression levels of Reg-3α and Reg-3γ transcripts post pancreatectomy. Though both the genes are upregulated, Reg-3γ upregulation seems to be relatively of a greater degree than Reg-3α and that, maximal expression is recorded on day 7 post Px with gradual decline through 14 and 21 days post Px. The degree of upregulation of both the genes is significantly greater in Px+ FRF mice than in Px mice. Apparently, the flavonoid rich fraction exerts an additive effect on transcriptional activation. The observed greater degree of ductal cell proliferation as assessed by BrdU incorporation and the greater number of duct associated nodular buds and the greater number of islets in Px mice exposed to FRF in comparison to non-exposed mice, agree well with the highly augmented Reg-3α and Reg-3γ expressions. Islet neogenesis would however require specific expression of endocrine precursor commitment genee to guide the neogenic precursor cells to differentiate into islet specific endocrine cells. Studies on embryonic development of pancreas have identified neurogenin-3 (Ngn-3) as the gene that commits the Hnf-1β$^+$ transition duct cells to endocrine progenitors (Solar *et al.*, 2009).

In the present study, Ngn-3 mRNA expression is significantly upregulated by 8 fold at day 7 post Px, which gets reduced to 6 fold by day 14 and to a mere 2 fold by day 21. In contrast, FRF treated Px mice show nearly 12 fold upregulation at day 7 post Px, and the upregulated expression persist at 5-6 fold high even at 14 and 21 days post Px. This would suggest islet neogenesis post Px in BALB/c mice exposed to FRF and this find excellent correlation with the observed duct associated islet neogenesis following Px and the relatively greater number and size of differentiating islets in FRF treated Px mice. Not only is Ngn-3 expression noticed at the time of endocrine

specification during pancreatic morphogenesis (Gu *et al.*, 2003; Mellitzer *et al.*, 2006; Solar *et al.*, 2009) but, also during islet neogenesis during pancreatic regeneration in the adult (Dor and Melton, 2008).

The importance of Ngn-3 in the specification of precursor cells for the various endocrine lineages in pancreatic islets is fully established by the reported inhibition of islet neogenesis by miRNA induced Ngn-3 gene silencing (Joglekar *et al.*, 2007a,b). It has also become clear from some recent studies that,models of diabetic animals in which intra-islet precursor or adult β-cell proliferation plays a primary role in β-cell regeneration, Ngn-3 expression is not important as, Ngn-3 inhibition was of no consequence and normal β-cell regeneration occurred (Lee *et al.*, 2006; Joglekar *et al.*, 2007a). It is also of interest to note that, a higher glucose level facilitates pancreatic endocrine cell development by potentiating the expression of Neuro-D, a downstream target of Ngn-3 (Guillemain *et al.*, 2007). Presumably, as the hyperglycemia characteristic of Px as in the present case can favour islet endocrine cell development by complimenting the function of Ngn-3. The higher and larger duration persistence of Ngn-3 expression in FRF treated mice as well correlatable with the noticed larger number and size of neogenic FRFtreated pancreas as substantiated by the documented greater immunoreactivity for insulin.

The greater insulin immunoreactivity in the islets of FRF exposed mouse pancreas again finds correlation with the recorded relatively lesser inhibition of Ins-1 and 2 proinsulin transcripts. The greater degree of inhibition of insulin biogenesis seen in Px mice is effectively minimized by FRF exposure. Apparently, treatment with FRF extract has significant favourable influence on insulin synthesis as seen by the relatively higher plasma insulin titres in FRF treated mice. This increasing pro-insulin mRNA expression and recovering insulin levels may suggest greater number

of β-cells as also evidenced by the greater immunoreactivity for insulin in FRF exposed mice, which may bear some relevance in the context of recently reported new function of Pdx-1 (Oliver-Krasinstri et al., 2009). According to their finding, the C terminus of Pdx-1 has a novel function of forming a molecular complex with Hnf6 and inducing the expression of Ngn-3 and, it also indirectly regulates ngn-3 expression by controlling the regulatory network of Sox-9, Foxa2, Hnf6 and Hnf1b. From this ability of Pdx-1 to upregulate the expression of Ngn-3 and also its known role in proliferating and differentiated β-cells, it is easily inferable that the presently observed greater number of islets and β-cells with the FRF supplementation is relatable with the greater Pdx-1 expression as substantiated by the immunocytochemical and qPCR data. This inference finds further substantiation by the herein recorded minimal glucagon positive cells and similar number of α-cells proliferation as detected by BrdU incorporation in both Px and Px + FRF mice.

Conclusion:

Overall, the present findings indicate islet neogenesis as the mode of β-cell regeneration in pancreatectomized BALB/C mice and provide evidence for flavonoidal rich fraction of OI extract to have enhancing influence on islet neogenesis and greater β-cell regeneration by as yet unknown influence on the genetic network controlling islet neogenesis and β-cell differentiation. The reports of Ogata et al. (2004) and Kojima et al. (2006) of the ability of coriophylene a Vinca alkaloid in inducing differentiation of pancreatic endocrine precursor cells and of Sidhu et al. (2010) of Rosiglitazone to promote β-cell regeneration from stellate cells are relevant in the present context. It is also clear from the present findings that, ductal cells can

serve as progenitors for islet neogenesis in response to appropriate triggering stimulation(s) generated by the stress of substantial pancreatic loss, by reverting to a plastic phenotype state similar to embryonic progenitors, as has been suggested by a working hypothesis extended by Bonner-Weir and Sharma (2010). This also over-rules the myth of resistance to nuclear reprogramming of fully differentiated cells and, as such, reprogramming of pancreatic exocrine cells has been adequately documented (Zou *et al.*, 2008). More focussed and reshaped experimental approaches need to be undertaken to fully fathom the cell types involved in reprogramming and the specific signals generated under various types of pancreatic stress and the underlying genome organisation that need to be attend for reprogramming, as also opined by Bukys and Jensen (2010).